



WENDY aims at unravelling the factors triggering social acceptance of wind farms through an in-depth analysis at three dimensions: social sciences and humanities, environmental sciences and technological engineering.

D3.1: Validated models for integrated life-cycle assessment on ecosystem services and biodiversity

WP 3: T3.1 & T3.2

Authors: Kvalnes, Thomas (NINA)*, Spielhofer, Reto (NINA)*, Hanssen, Frank (NINA), May, Roel (NINA)

NINA - Norwegian Institute for Nature Research, P.O. Box 5685 Torgarden, NO-7485 Trondheim, Norway

* - Shared first authorship



Funded by the
European Union

Funded by the European Union. Views and opinions expressed are however those of the author(s) only and do not necessarily reflect those of the European Union. Neither the European Union nor the granting authority can be held responsible for them.

Technical references

| | |
|---------------------|--|
| Project Acronym | WENDY |
| Project Title | Validated models for integrated life-cycle assessment on ecosystem services and biodiversity |
| Project Coordinator | CIRCE - Centro de Investigación de Recursos y Consumos Energéticos jperis@fcirce.es |
| Project Duration | October 2022 – September 2025 (36 months) |

| | |
|------------------------------|---|
| Deliverable No. | D3.1 |
| Dissemination level | PU – Public, fully open |
| Work Package | WP 3 - Energy landscape and environmental design: Environmental and technological impact assessment of wind energy |
| Task | T3.1 - Quantify direct and indirect LCA impacts from wind energy on biodiversity T3.2 - Map changes in ecosystem service benefits due to wind energy development |
| Lead beneficiary | 3. NINA |
| Contributing beneficiary/ies | 1. CIRCE , 4. EGP |
| Due date of deliverable | 30 September 2023 |
| Actual submission date | 26 September 2023 |

- PU – Public, fully open
- SEN – Sensitive, limited under the conditions of the Grant Agreement
- Classified R-UE/EU-R – EU RESTRICTED under the Commission Decision No2015/444
- Classified C-UE/EU-C – EU CONFIDENTIAL under the Commission Decision No2015/444
- Classified S-UE/EU-S – EU SECRET under the Commission Decision No2015/444

| v | Date | Beneficiary |
|-----|------------|-------------|
| 1.0 | 26/09/2023 | NINA |



Disclaimer of warranties

This project has received funding from the Horizon Europe Framework Programme (HORIZON) under Grant Agreement No 101084137.

This document has been prepared by WENDY project partners as an account of work carried out within the framework of the EC-GA contract no 101084137.

Neither Project Coordinator, nor any signatory party of WENDY Project Consortium Agreement, nor any person acting on behalf of any of them:

- (a) makes any warranty or representation whatsoever, express or implied,
 - (i). with respect to the use of any information, apparatus, method, process, or similar item disclosed in this document, including merchantability and fitness for a particular purpose, or
 - (ii). That such use does not infringe on or interfere with privately owned rights, including any party's intellectual property, or
 - (iii). That this document is suitable to any user's circumstance; or
- (b) assumes responsibility for any damages or other liability whatsoever (including any consequential damages, even if Project Coordinator or any representative of a signatory party of the WENDY Project Consortium Agreement, has been advised of the possibility of such damages) resulting from your selection or use of this document or any information, apparatus, method, process, or similar item disclosed in this document.



Executive summary

The Horizon Europe WENDY project is funded by the European Union research and innovation action programme under grant agreement number 101084137. The WENDY project will conduct multicriteria analysis of the technical, environmental, and social factors triggering the *Please In My Back Yard* (PIMBY) principle for wind technologies.

The positive effects of wind energy to produce renewable energy and mitigate the negative impacts of climate change, are accompanied with various impacts on humans and ecosystems locally. The cause of these effects are the large areas which are being occupied and transformed during construction and operation, which reduce the availability and suitability of areas for humans and wildlife. To understand factors that trigger acceptance for wind energy, as one of the main WENDY project goals, it is key to establish site-specific knowledge about the impacts on both, ecosystem services and biodiversity. While ecosystem services represent the utilitarian values of nature, biodiversity refers to the intrinsic values of nature.

This project report establishes a conceptual framework to integrate biodiversity and ecosystem service assessments (ESA) into a life cycle assessment (LCA) for onshore and offshore wind energy. LCA analyse the environmental impacts through the whole life cycle of wind farms and is useful for the assessments at different sites over heterogeneous landscapes. For biodiversity and ecosystem services the most direct and severe impacts are in-situ during the operational phase of the wind farms, which is the focus of this report.

For biodiversity the main impacts of operational wind farms can be given as habitat loss, collision risk, disturbance and barrier effects. We develop and adopt methods to quantify these impacts for birds and bats onshore and seabirds and marine mammals offshore. The methods requires that species distribution maps are available or made for a large region covering the site for a wind farm. Then the potentially disappeared fraction of species is calculated to quantify the impacts in a standardised and spatially explicit way. The second part of the report explains the impacts of wind energy on ecosystem services. Hereinafter, we present a mapping tool, integrated in a questionnaire to assess areas of ecosystem service values by people. This mapping tool allows capturing peoples' utilitarian view on the landscape. Analogically to the biodiversity assessment, the third part ends with the spatially explicit calculation of the impacts of wind energy on ecosystem services.

The combination of the loss of intrinsic (biodiversity) and loss of utilitarian (ecosystem service) due to wind energy is finally integrated into a net environmental performance index (NEP). The NEP serves as one of the KPI established in work package (WP) 3 of the WENDY project.



Table of contents

| | |
|---|-----------|
| List of Tables..... | 6 |
| List of Figures | 6 |
| 1 Life cycle assessment of wind energy on biodiversity and ecosystem services..... | 7 |
| 2 Impacts on Biodiversity | 10 |
| 2.1 Species and functional groups..... | 10 |
| 2.1.1 Birds | 10 |
| 2.1.2 Bats..... | 10 |
| 2.1.3 Marine mammals | 10 |
| 2.2 Species occurrence data | 11 |
| 2.3 Mapping species occurrence | 11 |
| 2.4 Connectivity | 12 |
| 2.5 Impact pathways..... | 13 |
| 2.5.1 Habitat loss..... | 13 |
| 2.5.2 Disturbance | 14 |
| 2.5.3 Collision | 16 |
| 2.5.4 Barrier | 16 |
| 3 Impacts on ecosystem services | 18 |
| 3.1 Impacts of wind energy on ecosystem services | 19 |
| 3.2 Mapping ecosystem service values..... | 21 |
| 3.2.1 PGIS combined with spatial Delphi..... | 22 |
| 3.2.2 Spatial extrapolation of ecosystem services..... | 25 |
| 3.2.3 Convergence zones of ecosystem services | 28 |
| 3.3 Integration of ESA into LCA | 29 |
| 3.3.1 Invariability-area relationship (IAR)..... | 29 |
| 3.3.2 The z-value as the shape of IAR | 30 |
| 3.3.3 Area lost for ecosystem services due to land occupation $A(O)$ | 30 |
| 3.3.4 Area lost for ecosystem services due to disturbance $A(D)$ | 31 |
| 3.3.5 Weighted PDF for ecosystem services..... | 31 |
| 4 Net environmental performance index | 32 |
| 5 Conclusion | 33 |
| 6 References | 34 |
| 7 Supplementary material | 44 |



List of Tables

Table 1: The midpoint effects of wind power on biodiversity and ecosystem services..... 8
 Table 2: Selected ecosystem services to map ecosystem service values with a spatial Delphi 20

List of Figures

Figure 1 System borders of the LCA wind power including on biodiversity and ecosystem services. 8
 Figure 2: Adapted ecosystem service cascade 18
 Figure 3: User interaction and data output (grey) of two spatial Delphi rounds. 22
 Figure 4: Detailed procedure and outputs (grey) of participatory mapping of each ES in round one of the spatial Delphi..... 23
 Figure 5: Screenshot of the introduction screen of the Spatial Delphi tool (9.8.23). 25
 Figure 6: Point sampling strategy and corresponding Maxent extrapolation..... 28
 Figure 7: Example of log-log scaled invariability – area relationship..... 30

1 Life cycle assessment of wind energy on biodiversity and ecosystem services

Renewable energy is being developed at a rapid pace to accommodate concerns regarding climate change effects and the emission of greenhouse gasses. Wind power plays a major role in this transition to renewable energy (Wiatros-Motyka et al., 2023), but the development and operation of wind farms can have negative impacts on biodiversity and ecosystem services (Buchmayr et al., 2022; Dai et al., 2015; Maxwell et al., 2022; May et al., 2020). The cause of these effects are the large areas which are being occupied and transformed during construction and operation, which reduce the availability and suitability of areas for humans and wildlife. The impacts may follow several pathways which may be difficult to assess, with different mechanisms at play for onshore and offshore wind farms (Dai et al., 2015; Maxwell et al., 2022; May et al., 2020).

Life Cycle Assessment (LCA) has been established as a standardized method to analyse the environmental impacts through the whole life cycle of potential stressors, such as wind farms. It has also been shown to be an appropriate tool to simultaneously assess multiple impacts and calculate environmental consequences in a spatial explicit manner (Verones et al., 2017). Thus, it is useful for the assessment of environmental impacts of wind farms at different sites over heterogenous landscapes. There are three stages to an LCA. First, the goal and scope of the assessment is defined to specify boundaries and which environmental effects that should be included. Second, a life-cycle inventory (LCI) is defined and established using available literature. It quantifies input and output data needed for the construction of a model for the flow of effects on the environment. Finally, a life-cycle impact assessment (LCIA) is carried out where LCI is used to evaluate the potential environmental impacts.

In the wind energy context, a LCA involves an assessment of both, the *effects* and *impacts* of wind energy infrastructures. The *effects* of wind energy infrastructure are described by midpoint indicators in the LCA, while the *impacts* of these effects on ecosystem services and biodiversity are described by endpoint indicators (Bare et al., 2000; Verones et al., 2017). Midpoint effects of wind energy, might be positive or negative, vary in temporal and geographical scale and include distant, indirect effects (*ex-situ*) or direct (*in-situ*) effects (Weidema et al., 2018). The LCA for wind farms can be divided into several phases (i.e. the manufactory, construction, operation and decommissioning; Figure 1). *Ex-situ* effects relate to all phases along the life cycle of the wind energy infrastructure which does not directly affect the site of the wind farm. By contrast, *in-situ* effects account for the changes in land use and other changes where the wind energy infrastructure is sited. Thus, these effects are contained in the operational phase and directly impacts biodiversity and ecosystem services. For wind energy, *in-situ* midpoint indicators encompass land occupation (i.e. habitat loss), collision mortality, disturbance and barrier effects on wildlife or humans' use of natural areas (Table 1). Endpoint indicators enable the quantification of these midpoint effects as impacts on the three dimensions of human health, biodiversity and ecosystem services (Callesen, 2016; May et al., 2021). For biodiversity, endpoint impacts quantify the changes in (often the loss of) species richness and thus refer to the intrinsic value of biodiversity. This is usually quantified as the potentially disappeared fraction (PDF) of species, which describe the loss of species richness following impacts which cause the loss of suitable habitat (May et al., 2020; Verones et al.,



2017). By contrast, LCA endpoint impacts on ecosystems services (ES) quantify the changes of the utilitarian values of nature. Consequently, the impacts on ES caused by wind energy development describe the changes in how and where humans benefit from nature. To gain a holistic understanding of the costs and benefits of wind energy infrastructure, research and practice should aim to integrate accounts of biodiversity and ecosystem service assessment (ESA) within LCA (Rugani et al., 2019; Hardaker et al., 2022; Callesen, 2016).

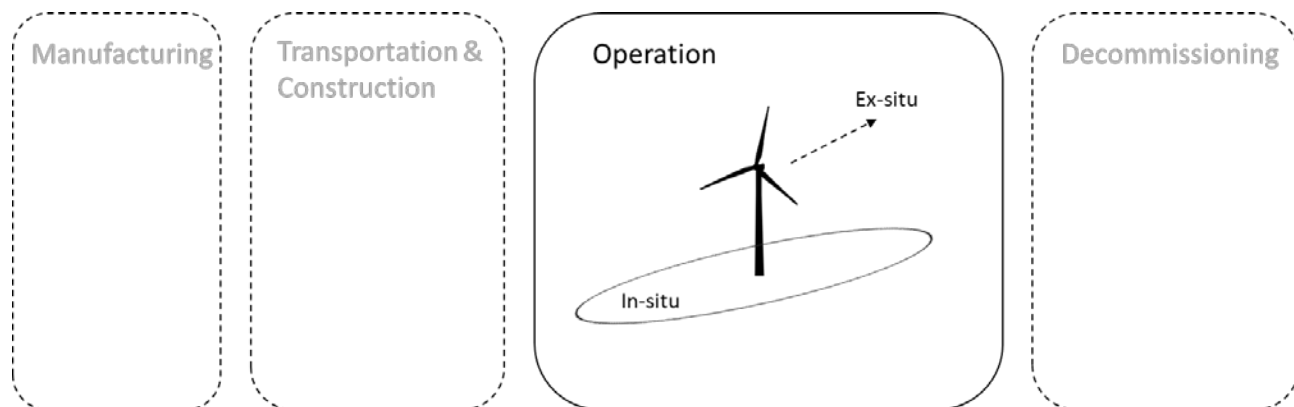


Figure 1 System borders of the LCA wind power including on biodiversity and ecosystem services.

Table 1: The midpoint effects of wind power on biodiversity and ecosystem services.

| Midpoint effects | Description |
|--------------------------------|--|
| Land occupation (habitat loss) | Physical, direct alterations of land cover on the footprint of the fundaments and maintenance areas of wind turbines. These areas might be larger during the construction phase (including also temporarily affected areas) and smaller during the operational phase (only including permanently affected areas) after revitalization. |
| Collision risk | The rotating blades of the turbines poses a risk of collision for birds and bats. |
| Disturbance | Alteration of a landscape’s physical or acoustic appearance through artificial installation. |
| Barrier effects | Fragmentation of habitats due to the land occupation and disturbance from wind turbines. Influences on movement behaviour of species or people. |

This deliverable conceptually describes the integration of biodiversity and ESA in an LCA for wind energy infrastructure and summarizes the steps performed in work package (WP) 3, task 3.1 and 3.2 of the WENDY project. To do so, both assessments focus on the same set of impact pathways of wind energy

and use the same concepts to account in spatial explicit manner for PDF. In addition, both assessments focus on the operational phase of the wind energy production (Figure 1). Chapter 6 describes the impact analysis on biodiversity (T.3.1), while chapter 7 does so for ES (T.3.2). The impact analysis of both dimensions leads to a spatially explicit understanding of trade-offs and synergies in the human-environment interactions regarding wind energy production. Finally, chapter 8 elaborates a net environmental performance (NEP) indicator for biodiversity and ecosystem service impacts, that enhance comparability between different project sites.



2 Impacts on Biodiversity

Assessing the impact of operational wind farms on biodiversity requires holistic methods which may collect the impacts of all the important impact pathways for different groups of species. LCIA methods for assessing habitat loss, collision, disturbance, and barrier effects have recently been developed for birds onshore (May et al., 2020; May et al., 2021). We present these and in addition, we adapt and generalize these methods for birds offshore, bats and marine mammals. We focus on species of bats and birds found on the European continent and birds and marine mammals found in selected marine regions; the Norwegian economic zone, the North Sea and Skagerrak for this report. However, the methods which are developed are general and should be applicable to any area for these groups of animals given that it is sufficiently large to cover a relevant range of environmental conditions. Polygons for the boundaries for countries within which onshore analyses are performed can be downloaded from geoBoundaries (geoboundaries.org). Similarly, marine regions can be downloaded from Marine regions (marineregions.org).

2.1 Species and functional groups

2.1.1 Birds

There are 545 species of birds regularly occurring (breeding and/or wintering) in Europe (BirdLife International, 2021). Groups of species were made based on functional similarity and taxonomic relationships (Table S1, May et al., 2021). The number of species in each group ranged from 16 for owls to 89 for insectivorous songbirds. Offshore we include all species of gulls, seabirds, raptors, waterbirds and waterfowl which are commonly found in the marine or coastal area.

2.1.2 Bats

The 55 species of bats found in Europe according to EUROBATS were grouped according to the duration and bandwidth of echolocation calls into short-range echolocators (SRE), mid-range echolocators (MRE) and long-range echolocators (LRE) (Supplementary material Table S2, Brenda et al., 2008; Collen, 2012; Frey-Ehrenbold et al., 2013; Froidevaux et al., 2023; Holderied et al., 2005; Holland et al., 2004; Obrist et al., 2004). These different echolocation groups are assumed to have different ranges for perception and defines different foraging guilds of functionally similar species.

2.1.3 Marine mammals

In the focal area, 19 species of marine mammals can be found (Supplementary material Table S3, Bjørge et al., 2010; Reid et al., 2003), which include 17 Cetaceans and two true seals. Marine mammals were classified into three functional groups based on taxonomy and functional similarities; baleen whales, toothed whales and seals (Supplementary material Table S3).



2.2 Species occurrence data

For birds and bats, presence data will be downloaded for the period 2000 to 2022 from the Global Biodiversity Information Facility (GBIF, gbif.org). For onshore analyses, the data will be filtered to only include observations of animals onshore and records with position uncertainty larger than 0.5 km will be excluded. For offshore analyses, that on seabirds will be filtered to only include observations at sea, and records with position uncertainty larger than 5.5 km will be removed. We do not consider seasonal migration specifically in the analyses and include all records throughout the year.

For marine mammals we can download presence data from the Global Biodiversity Information Facility (GBIF, gbif.org) and the Ocean Biodiversity Information System (OBIS, obis.org). The data will be restricted to records collected between 2000 and 2022 and filtered to only include only observations of animals at sea. Records with position uncertainty larger than 5.5 km will be removed from the data set.

2.3 Mapping species occurrence

Modelling of the spatial distribution of each species will be based on occurrence records and a set of ecological relevant environmental variables using Maxent software (version 3.4.3, Phillips et al., 2017). We will use 10 000 background samples (without replacement), default regularization and allow linear, quadratic, product and hinge features to be used to fit the models. However, to avoid using too large proportions of raster cells as background we limit the number of background samples to maximum c. 50 % of the available cells in a raster. This will e.g. reduce the number of background samples to 7000 for the offshore area covered in the report. Estimates of the intensity of occurrence records (Maxent's "raw" output) will be transformed to occurrence probability using the complementary log-log (cloglog) transformation (Phillips et al., 2017) to have an index of the mean probability of presence.

Species occurrence data often exhibits a strong geographic bias, introduced by variation in accessibility and interest of observers between areas (Dennis & Thomas, 2000; Kadmon et al., 2004). Thus, we apply two methods to avoid an effect of sampling bias on the resulting species distributions. First, we will apply systematic sampling of records by constructing a 1 km² (onshore) or 10 km² (offshore) grid across the study area and select one record of each species for each cell in the grid (Fourcade et al., 2014). At this point, species with less than 50 records will be excluded from the data set. Second, we will use target-group background when running the Maxent-models (Phillips et al., 2009), which replicate the spatial bias in occurrence records for the background samples. These methods have been shown to outperform other alternative methods for bias correction in species distribution models (SDM, Barber et al., 2022; Fourcade et al., 2014). To generate the target group background, we used the occurrence records for all species with 2D kernel density estimation and normalized (0,1) the resulting raster maps to create a probability surface over the study area used when drawing background points (Barber et al., 2022).

For birds onshore, there are seven environmental variables which will be included in the analyses (May et al., 2021). Including annual mean temperature (°C), temperature seasonality (standard deviation × 100), annual precipitation (mm), precipitation seasonality (coefficient of variation) downloaded from World climate variables (worldclim.org, Fick & Hijmans, 2017). In addition, Corine land cover 2018



downloaded from the Copernicus programme (land.copernicus.eu) and elevation (m) downloaded from GEBCO (gebco.net). Distance to sea will be calculated from the European coastline downloaded from EEA (eea.europa.eu/data-and-maps/data/eea-coastline-for-analysis-2).

For bats, we selected nine environmental variables which are likely to predict the distribution of bats (Jaberg & Guisan, 2001; Michaelsen, 2016; Scherrer et al., 2019). In addition to the seven environmental variables used for birds we also include the mean temperature of the warmest and coldest quarter downloaded from World climate variables (worldclim.org, Fick & Hijmans, 2017).

For birds offshore and marine mammals, environmental variables selected for the analyses included annual mean sea-surface temperature ($^{\circ}\text{C}$), annual mean surface salinity (PSS), annual mean primary productivity ($\text{g}\cdot\text{m}^{-3}\cdot\text{day}^{-1}$, carbon in sea water) and annual mean current velocity ($\text{m}\cdot\text{s}^{-1}$) downloaded from the Bio-ORACLE (Assis et al., 2018; Tyberghein et al., 2012). In addition, bathymetry and seabed slope were included. Bathymetry data can be downloaded from GEBCO (gebco.net) and seabed slope can be calculated from the bathymetry data. These variables have earlier been shown to be important for predicting the distribution of seabirds and marine mammals (Correia et al., 2021; Engler et al., 2017). All environmental variables will be resampled to a resolution of 1 km^2 (onshore) or 10 km^2 (offshore) identical to the grid for the occurrence data, using the spatial reference system ETRS89, LAEA (EPSG: 3035).

Species richness for each functional group k will be estimated by combining (stacking) the predicted species distribution maps to estimate relative probability of presence (Grenie et al., 2020). The resulting group-wise maps shows $S_k P_{k,i}$ for each site i , where S_k is the number of species in group k and $P_{k,i}$ is a score (between 0 and 1) that is proportional to the mean probability of presence for species in group k at site i (Phillips et al., 2017). Hence, this measure of species richness accounts for the suitability of the habitat for each species which affects the probability of occurrence at a given site.

2.4 Connectivity

Connectivity across the landscape will be modelled for each species applying circuit theory in the Omniscape (version 0.5.8, Landau et al., 2021; McRae et al., 2016) and Circuitscape packages (version 5.12.3, Anantharaman et al., 2020; McRae et al., 2008) using Julia software (version 1.6.7, Bezanson et al., 2017). This approach predicts omni-directional connectivity among every pair of locations in the landscape by iteratively applying Circuitscape to every cell through the species distribution maps and calculating cumulative current flow (McRae et al., 2016). The inverse species distribution maps will be used as resistance rasters and source strength will be set equal to the species probability of presence in Omniscape. Thus, habitat suitability ($P_{k,i}$) measures the conductance to movement across the landscape. The average cumulative current flow ($C_{k,i}$) for each group can then be calculated and normalized (0,1) to aggregate them into connectivity maps for each functional group ($S_k C_{k,i}$).



2.5 Impact pathways

The LCA impact of wind-power farms during the operational phase on species richness is estimated as the potentially disappeared fraction of species (PDF, May et al., 2021; May et al., 2020). This is a relative measure of the potential loss of species richness from a reduction in the area available at a given site i ($A_{new,i} = A_{org,i} - A_{lost,i}$) using the classical species-area relationships (SAR) (Tjørve et al., 2021). May et al. (2020) and May et al. (2021) developed methods for the four main impact pathways of wind farms in birds, 1) habitat alterations (H), 2) disturbance (D), 3) collisions (C), and 4) barrier effects (B). Here we generalize these methods to any map resolution and overlapping impact areas for different wind turbines. Then we adapt the methods to bats, birds offshore and marine mammals, and apply them to the raster maps of species richness estimated using SDMs. Collisions are not quantified for marine mammals as the risk of entanglement have been suggested to be very low given that cables and mooring lines are often taut and of large diameter (Maxwell et al., 2022).

Let a wind farm f have wind turbines $w = (1, \dots, l_f)$. For impact pathway X in functional group k , each wind turbine is defined by a polygon $F(X)_{k,f,w}$ with the shape of a circle and centroid at its coordinates (x, y) . The area occupied by the polygon for a wind turbine $A(X)_{lost,k,f,w} = a(F(X)_{k,f,w})$ is determined by the extent (radius) of the impact, and the polygon for the total area impacted for wind farm f is given by the union of the polygons of all wind turbines $F(X)_{k,f} = \bigcup_{w=1}^{l_f} F(X)_{k,f,w}$. The area lost for cell i in a raster map through impact pathway X can now be given by $A(X)_{lost,k,f,i} = a(F(X)_{k,f} \cap R_i | F(X)_{k,f} \cap R_i \neq \emptyset)$, where R_i is a polygon for cell i with area $A_{org,i}$. Then the PDF for group k at cell i can be estimated as

$$PDF(X)_{k,f,i} = \frac{S_k P_{k,i} \left(1 - \left(\frac{A_{org,i} - A(X)_{lost,k,f,i}}{A_{org,i}} \right)^z \right)}{\sum_{i=1}^n S_k P_{k,i}}, \quad (1)$$

where the exponent z is taken to be 0.21 (95 % CI = [0.19, 0.22]) or 0.26 (95 % CI = [0.24, 0.27]), the continental-scale SAR estimate for, respectively, birds and mammals in Eurasia (Storch et al., 2012), and $X = (H, D, C, B)$. For a wind farm f , the PDF for group k through an impact pathway is calculated as the sum of the cell-wise values, $PDF(X)_{k,f} = \sum_i PDF(X)_{k,f,i}$. The PDFs can further be aggregated across functional groups, $PDF(X)_f = \sum_k PDF(X)_{k,f} \sum_i S_k P_{k,i} / \sum_i S P_i$, impact pathways, $PDF_{k,f} = \sum_X PDF(X)_{k,f}$ or both, $PDF_f = \sum_X PDF(X)_f$. PDF_f then quantifies the total impact of a wind farm on the functional groups of species included in the analysis.

2.5.1 Habitat loss

2.5.1.1 Birds and bats onshore

Habitat loss for birds and bats onshore is determined by the area required for the foundation of a turbine and the surrounding infrastructure, which increases with the MW capacity of the turbine (Denholm et al., 2009; May et al., 2020). The directly impacted area (permanent changes) and the indirectly impacted area (temporary changes) have been found to be 0.003 km²/MW (95 % CI = [0.0026, 0.0033]) and 0.007 km²/MW (95 % CI = [0.0062, 0.0078]) (Denholm et al., 2009). The area lost to each wind turbine can then be given as $A(H)_{lost,k,f,w} = a_{EP} EP_w$, where a_{EP} is the value for direct or indirect impact in km²/MW and EP_w is the electric power of wind turbine w (May et al., 2020).

2.5.1.2 Birds and marine mammals offshore

Habitat loss for birds offshore and marine mammals is determined by the area of the seabed and/or ocean habitat which is occupied by the foundation, anchors, mooring lines and cables for each wind turbine. The area lost to each wind turbine can be given as $A(H)_{lost,k,f,w} = a_{f,w} + a_{a,w}n_{a,w} + a_{m,w}n_{m,w} + a_{c,w}$, where $a_{f,w}$ is the area of the ocean and/or seabed occupied by the foundation, $a_{a,w}$ and $n_{a,w}$ are the area of seabed occupied and number of anchors, $a_{m,w} = r_{m,w}d_{m,w}$ and $n_{m,w}$ are the area and number of mooring lines for each wind turbine, calculated from the mooring radius $r_{m,w}$ and the diameter of the mooring lines $d_{m,w}$, and $a_{c,w} = r_{c,w}d_{c,w}$ is the area occupied by the electrical cable between wind turbines, calculated from the diameter of the cable $d_{c,w}$ and the average inter-turbine distance $r_{c,w}$. An estimate of the mooring radius can be derived based on knowledge of ocean depth. The ratio mooring radius/depth (R/D) is often around 1.4 for taut systems and decreases exponentially with depth for the commonly used catenary systems (50m: R/D = 10, 100m: R/D = 9, 150m: R/D = 5, 200m: R/D = 4, 400m: 3, 600m: 2, 1000m: R/D = 1.5, Ma et al., 2019).

2.5.2 Disturbance

In addition to habitat loss, a species may be deterred from using a larger area surrounding each wind turbine due to disturbance effects. The strength of this effect may vary between species such that a proportion of species in each group k may be lost from the area. We quantify the avoidance effect by the disturbance distance (d) for each species (in km). The disturbance distance can be obtained from the literature for birds and bats and will be estimated based on the effect of the noise emitted from the wind turbines for marine mammals.

2.5.2.1 Birds and bats

For birds onshore and offshore, flight initiation distance obtained from the literature were used as a measure of disturbance distance (d) for each species (all sources are provided in the full data set, May et al., 2020). The maximum distance was taken if more than one estimate was found per species.

For bats, the disturbance distance (d) was taken to be the maximum distance from a wind turbine with evidence for reduced bat activity (Barre et al., 2018; Ellerbrok et al., 2022; Gaultier et al., 2023; Leroux et al., 2022; Minderman et al., 2017). When multiple estimates were available from different sources, species level estimates were chosen over genus level estimates and genus level estimates were chosen over guild level estimates. The maximum was taken if several estimates were available at the preferred level. If no estimate was available for a species, the average of species within its genus or family was used. Estimates of disturbance distance was missing for the families Pteropodidae, Emballonuridae, Miniopteridae, Molossidae with a total of five species in Europe.

The area lost to each wind turbine can be estimated by $A(D)_{lost,k,f,w} = \pi(D_k d_{k,max})^2$ for birds and bats (May et al., 2020). Here $d_{k,max}$ is the maximum disturbance distance and D_k is the disturbance factor for group k . The disturbance factor is estimated as

$D_k = \int_{d=0}^{d_{k,max}} \frac{1-1/(1+e^{\beta(d-\bar{d}_k)})}{d_{k,max}} d\theta$ (May et al., 2020), where $\beta = \frac{\log((2-\alpha)/\alpha)}{d_{k,min}-\bar{d}_k}$, $\alpha=0.1$ and $d_{k,min}$ is the minimum and \bar{d}_k the mean of d in group k .

2.5.2.2 Marine mammals

For marine mammals, an important factor causing disturbance is the underwater noise generated by operating wind turbines. The disturbance distance for each species is estimated as the distance required for the noise emitted from a wind turbine to fall below a defined acoustic threshold for behavioural responses due to continuous noise. We use the level B criterion of 120 dB re 1 μ Pa root-mean-squared defined by the National Oceanic and Atmospheric Administration (NOAA) (Gomez et al., 2016; see also Southall et al., 2007). Marine mammals can be classified into hearing groups with similar auditory sensitivity, for which the disturbance distance will be different. We use the classification in Southall et al. (2019), with, low-frequency cetaceans (LF), high-frequency cetaceans (HF), very high-frequency cetaceans (VHF) and Phocid carnivores (seals) in water (PCW, see Table S3). The auditory frequency weighting function for species in each of these groups can be given by (Southall et al., 2019)

$$W(f) = C + 10\log_{10} \left(\frac{(f/f_1)^{2a}}{(1+(f/f_1)^2)^a(1+(f/f_2)^2)^b} \right), \quad (2)$$

where f is the frequency of a target sound in kHz, f_1 is the lower frequency at which the function begins to change from flat, and f_2 is the upper frequency at which the function begins to change from flat, a and b are the lower frequency and upper frequency exponents which define the rates of decline and C is a constant (parameter estimates for each hearing group is given in Supplementary material Table S4).

The total sound pressure level (dB re 1 μ Pa root-mean-squared) of the noise emitted from a wind turbine w increase with its nominal electric power (EP_w , in MW) (Stöber & Thomsen, 2021; Tougaard et al., 2020). For wind turbine w , we estimate the total broadband sound pressure level of noise at 100 meter distance and 10ms wind strength by $dB_{at r_1}(EP_w) = 109 \pm 1.7 - 23.7 \pm 3.1 \log_{10} \left(\frac{100m}{100m} \right) + 18.5 \pm 5.8 \log_{10} \left(\frac{10ms}{10ms} \right) + 13.6 \pm 3.8 \log_{10} \left(\frac{EP_w}{1MW} \right)$ (Tougaard et al., 2020). 95 % confidence intervals for the sound pressure level can be estimated using the estimated standard error for the electric power effect in the equation. We then take the maximum broadband sound pressure levels as an approximation for the spectral pressure level at the peak frequency (Stöber & Thomsen, 2021; Tougaard et al., 2020).

Transmission loss (ΔL) was calculated using the practical spreading loss model, $\Delta L = \kappa \log_{10}(r/r_1)$, where r is the distance (m) at which the transmission loss is estimated, r_1 is the distance at which the sound pressure level is measured (here estimated at 100 m) and we set $\kappa = 23.7$ as found by Tougaard et al. (2020). Generally, κ is the mode of spreading loss, where the rate of loss decreased from the spherical ($\kappa = 20$) to the cylindrical model ($\kappa = 10$) (Stöber & Thomsen, 2021). Rewriting this equation, and applying the auditory weighting function and acoustic threshold, the disturbance distance for a species (in km) can then be calculated by $d = (100 \times 10^{((dB_{at r_1}(EP_w) + W_{k,j}(f) - dB_{acoustic threshold})/\kappa)}) 1000^{-1}$. The peak frequency (Hz) of underwater noise from offshore wind turbines have been found to have a range of 14-400 Hz (Tougaard et al., 2020). Hence, we set $f = 0.400$ kHz which will be the frequency most audible to marine mammals.

The area lost to each wind turbine can then be estimated by $A(D)_{lost,k,f,w} = \pi \bar{d}_k^2$ for marine mammals (May et al., 2020). Here \bar{d}_k is the mean disturbance distance for group k .

2.5.3 Collision

Species of birds and bats which utilize the area within the rotor swept zone around each wind turbine have a risk for collision both onshore and offshore. Species-specific estimates of Poisson-distributed collision rates (*rate*) with lower and upper 95 % credible intervals were collected from Table S4 in Thaxter et al. (2017). However, collision rates for many marine birds, especially seabirds, were missing from the literature. Hence, for 19 species we estimated collision rates based on a log-log regression of collision risk index (Furness et al., 2013; Wade et al., 2016) and collision rate (Thaxter et al., 2017). This was done using the 37 species for which a collision risk index was available in Furness et al. (2013) and Wade et al. (2016). Among these species, 18 had estimates of both collision risk and collision rate and their relationship was estimated to be $rate = 0.0113 \times risk^{0.6046}$, $R^2 = 0.814$. For two species the collision risk index was set to 0 as they seldomly are recorded at flight heights within the rotor swept zone and we added a small quantity (0.01) to the risk to allow log-transformation and account for the non-zero proportion of higher flights (Furness et al., 2013). The collision rates for all species were then used to estimate the probability of at least one collision occurring per year (R_k), by $R_k = 1 - e^{-rate_k}$, where $rate_k$ is the average collision rate for group k . We could quantify the uncertainty in our estimated PDF using lower and upper estimates of R_k . The area lost to each wind turbine for collision effects can then be given as $A(C)_{lost,k,f,w} = R_k \pi r_{f,w}^2$, where $r_{f,w}$ is one-half the rotor diameter (in km, May et al., 2020).

2.5.4 Barrier

Wind farms may cause a barrier effect, resulting in an increase in travel distance for migrating animals that avoid going through the disturbed area (Dierschke et al., 2016). Barrier effects are quantified using the method developed in May et al. (2021), where the increase in the energetic expenditure is proportional to the disturbance caused by building a wind turbine at a given site. The total energy requirement for migration (M_k) in group k is quantified based on the energetic requirement (a_k) per km travelled and the distance travelled per season (l_k) multiplied by 2 to account for spring and autumn migration, $M_k = 2a_k l_k$. The area of impact for each wind turbine set equal to the impacted area from disturbance multiplied by the total energy requirement for migration, $A(B)_{lost,k,f,w} = M_k A(D)_{lost,k,f,w}$ (May et al., 2021). Then we use the connectivity map instead of the species richness map and replace $P_{k,i}$ by $C_{k,i}$ in equation 1, such that the PDF for group k at cell i can be estimated as (May et al., 2021)

$$PDF(B)_{k,f,i} = \frac{S_k C_{k,i} \left(1 - \left(\frac{A_{org,i} - A(B)_{lost,k,f,i}}{A_{org,i}} \right)^Z \right)}{\sum_{i=1}^n S_k C_{k,i}} \quad (3)$$

2.5.4.1 Birds and bats

The energetic requirement per km travelled per season is estimated for each species given by $a = \frac{F_w}{F_s BMR_s}$ (Somveille et al., 2018), where F_w is the flight power (J/s), F_s is the flight speed (m/s) and BMR_s is the basal metabolic rate (J) over a whole season. The average of a across species in functional group k is used as the estimate of a_k . Somveille et al. (2018) found that the energetic requirement per km travelled for birds was given as $a = 6.07 \times 10^{-5} m^{-0.01}$, where m is body mass (after scaling from g to kg). Body

mass for all species was obtained from Tobias et al. (2022) and migration distances was obtained from Vincze et al. (2019) and supplemented with data from other literature for seabirds and gulls (all sources area provided in the full data set).

For bats, the allometric relationships for flight power and speed have been found to be $F_w = 55.7m^{0.80}$ and $F_s = 8.4m^{0.08}$ (Hedenstöm et al., 2009), where m is the mean body mass (kg). The allometric relationship of BMR (kJ/h) in bats has been found to be $BMR = 8.483m^{0.707}$ (after scaling body mass from g to kg, McNab, 2008). Hence, $BMR_s = 37.05 \times 10^6 m^{0.707}$ after converting BMR to J/s and multiplying by the number of seconds in 6 months (i.e. $\sim 15\,724\,800$ seconds a season). Using the equations for F_w , F_s and BMR_s , the equation for the energetic requirement per km travelled for bats can then be given as $a = 1.79 \times 10^{-4} m^{0.013}$. The distance travelled per season l_k was collected from Froidevaux et al. (2023) and Hutterer et al. (2005) and mean body mass m for each species was collected from Ancillotto et al. (2020), Brenda et al. (2008), Froidevaux et al. (2023) and the PanTHERIA database (Jones et al., 2009).

2.5.4.2 Marine mammals

For marine mammals, the energetic requirement per km travelled is estimated by $a = \frac{COT}{BMR_s}$ (see Somveille et al., 2018), where COT is the cost of transport (J/m) and BMR_s is the basal metabolic rate (J) over a whole season. The allometric relationship of COT has been found to be $COT = 7.79m^{-0.29}$ in marine mammals, where m is the body mass (kg, Williams, 1999). The allometric relationship of BMR (kJ/h) with body mass in seals (order Carnivora) and whales (order Cetacea) are different and have been found to be $BMR = 11.812m^{0.707}$ and $BMR = 31.473m^{0.707}$ (after scaling body mass from g to kg, McNab, 2008). Hence, we have $BMR_s = 51.60 \times 10^6 m^{0.707}$ for seals and $BMR_s = 137.48 \times 10^6 m^{0.707}$ for whales after converting BMR to J/s and multiplying by the number of seconds in 6 months (i.e. $\sim 15\,724\,800$ seconds a season). Thus, the equation for the energetic requirement per km travelled can then be given as $a = 1.51 \times 10^{-4} m^{-0.997}$ for seals and $a = 5.67 \times 10^{-5} m^{-0.997}$ for whales. The average of a across species in group k is used as the estimate of a_k . Estimates of body mass (m) was collected from the PanTHERIA database (Jones et al., 2009) and the migration distance (l_k) was collected from published literature based on records of the maximum movement range (de Boer et al., 2013; Dietz et al., 2013; Foley et al., 2021; Genov et al., 2012; Kettemer et al., 2022; Lydersen et al., 2020; Matthews et al., 2011; McConnell et al., 1999; Miller et al., 2015; Nawojchik et al., 2003; Olsen et al., 2009; Rasmussen et al., 2013; Read & Westgate, 1997; Robinson et al., 2012; Sampson et al., 2012; Stavenow et al., 2022; Steiner et al., 2012; Torres-Florez et al., 2015; Vikingsson & Heide-Jørgensen, 2015).

3 Impacts on ecosystem services

This chapter reflects on the spatially explicit ecosystem service assessment (ESA) and the estimation of impacts on ecosystem services (ES) through wind energy, adapting methods for LCIA developed in chapter 6 for biodiversity.

ES are defined as ecological products and processes that enable human survival and well-being (Costanza, 2020). Thus, ES are the nexus between the natural and socio-economic environment, conceptually described with the cascade model (Figure 2).

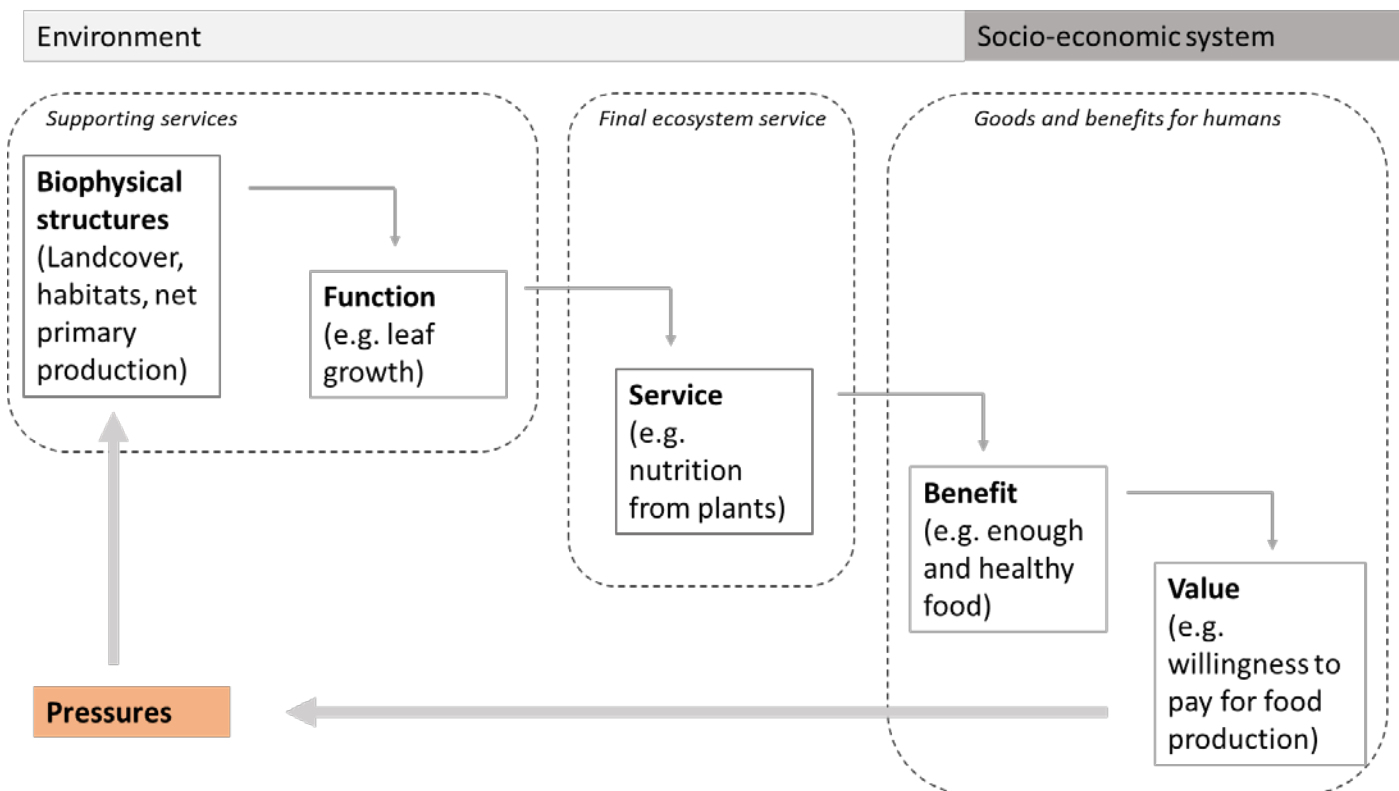


Figure 2: Adapted ecosystem service cascade

Biophysical structures, processes (habitats) and functions are located on the left side of the cascade. On the right side is the socio-economic system, which reflects the human demand for specific ES and finally their valuation. The model describes the pathway from ecological structures, the ecosystems, towards human well-being. However, the cascade is not one-way as it shows human demand for ES values as driving forces for pressures on structures and functions. These pressures have direct feedback in the cascade and influence the benefits and values people gain from nature.

Facing the global climate change, renewable energy production is critical to reduce greenhouse gas emissions (particularly carbon dioxide, CO₂; Smol, 2022). Consequently, the human demand for energy resources provided by wind, water, solar or biomass, representing the right side of the cascade model, increased significantly over the last two decades (IEA, 2022). However, an enhanced demand for

renewable energy, evolves pressures and impacts on the environment – the left side of the cascade. In addition, the demand for renewable energy will not only trigger environmental pressures, but it will also lead to spatial and temporal trade-offs with other ecosystem service demands. Particularly for trade-off analysis, ESA have been shown as a useful tool (De Luca Peña et al., 2022). Therein, ESA qualify and quantify the cause (i.e., more wind energy demand), the impacts on ecosystems and through the cascade the change in values human gain from ES. Particularly for renewable energy production a noticeable amount of international, peer-reviewed literature applies the ESA method (see Picchi et al., 2019 for an overview). Besides physical models to map and quantify ES, integrative approaches have been proposed to better consider the right side of the cascade by analysing people's assessment of ES values (Costanza, 2020). Thus, to better understand how groups of people evaluate different ES values, section 3.2 describes the application of a participatory geospatial Delphi tool to map people's perceived values of ES.

While ESA focus on the value people gain from ecosystems, the life-cycle assessment (LCA) methodology focuses on the human activity and multiple cause-effects or impact pathways (De Luca Peña et al., 2022; Rugani et al., 2019). Therefore, section 3.3 reflects on the concept to integrate ESA and LCA to account for the impact of wind energy on ecosystem services.

3.1 Impacts of wind energy on ecosystem services

To map ecosystem services in the context of wind energy impact, we adapt the common international classification of ecosystem services (CICES V5.1; Haines-Young & Potschin, 2018). CICES is widely used in different research fields and by national and international statistical divisions. Moreover, the CICES classification forms the basis of the ES mapping framework to support EU's Biodiversity strategy 2020. The application of an international standard leads to measurable and comparable indicators for final ecosystem services from which benefits for individuals and the whole society are derived (Boyd & Banzhaf, 2007). CICES provides a hierarchical structure of ES in sections, divisions, groups and classes. On the most detailed class level, CICES V5.1 covers 60 biotic and 32 abiotic ES with general descriptions of the services (<https://cices.eu>).

However, within an integrated ESA, where local people are asked to map and value ES, the ES classes need to be aggregated and the descriptions must be translated into general, local understandable terms and language. As a first aggregation level we used the CICES sections, that consist of three broad categories; provisioning, regulating/maintaining and cultural ecosystem services. For each of the CICES sections we developed a second aggregation level, so that each represents important aspects of impacts caused by wind energy. This second aggregation is based on a literature review of Picchi et al. (2019), including 38 peer-reviewed publications that applied ESA within the context of wind energy development. The authors categorized each publication into one or several CICES groups affected by wind energy development. Finally, we used the relative number of publications (column relevance in table 2) as a basis to derive the second aggregation of ecosystem services including in the mapping procedure. Although this measure is not representative, it indicates that impacts of wind energy on cultural ES is the most frequently analysed group, followed by the impacts on habitat and biodiversity.

Table 2: Selected ecosystem services to map ecosystem service values with a spatial Delphi

| Ecosystem service | CICES section | CICES group combinations | Brief description as landscape values "Places ..." | Relevance ¹ | Onshore | Offshore | Main LCA midpoint effects on ES |
|--------------------------------------|---------------|---|---|------------------------|---------|----------|--|
| Aesthetical values | Cultural | | ...that show the beauty of nature and landscapes. | 0.88 | x | x | Disturbance ² and land-occupation |
| Cultural or symbolic values | Cultural | Intellectual, symbolic, spiritual, cultural | ...that represents a high value for local culture or history or might serve personal spiritual values | - | x | x | Disturbance |
| Recreation | Cultural | Physical interaction, recreation, community activities | ... where people can spend time together or practice outdoor activities. | 0.31 | x | x | Disturbance and land-occupation |
| Regulation of atmospheric conditions | Regulating | Atmospheric conditions compositions | ... that help to regulate the temperature and store greenhouse gases. | 0.19 | x | | Land-occupation |
| Prevention of natural hazards | Regulating | Regulation of baseline flows and extreme events | ... that prevent people and infrastructure from floods, avalanches, or mass flows. | 0.08 | x | | Land-occupation |
| Farm products | Provisioning | Cultivated animals and plants (terrestrial & aquatic), reared animals for nutrition | ... that provide the potential to cultivate plants and animals for nutrition. | 0.16 | x | x | Land-occupation |
| Wild products | Provisioning | Wild animals and plants for nutrition | ... that are good for hunting or collecting of plants for | - | x | x | Disturbance and land-occupation |

¹ Relevance refers to a literature review of Picchi et al. (2019), indicating the relative number of papers covering a specific ecosystem service group.

² Visual & acoustic effects

| | | | | | | | |
|------------------|--------------|---------------------------------------|---|------|---|--|-----------------|
| | | | nutrition (berries mushrooms) ³ | | | | |
| Potable water | Provisioning | Surface water for nutrition | ... that provide clean potable water for drinking or irrigation. | 0.04 | x | | Land-occupation |
| Natural products | Provisioning | Fibres from plants, abiotic materials | ... where wood can be harvested or stones, sand can be extracted for building or producing industrial products. | 0.08 | x | | Land-occupation |

As defined in chapter 1, this study focusses on in-situ LCA-midpoint effects during the operational phase of a wind farm (Table 1). Thus, Table 2 also indicates the main midpoint effects of wind energy production for each ecosystem service. The different midpoint effects are considered in the impact calculation in section 3.3. To use the ES in a participatory mapping approach (Section 3.2), we adapted a short description of the ecosystem services as landscape values from another participatory mapping study (Stahl Olafsson et al., 2022).

3.2 Mapping ecosystem service values

While biodiversity mapping (section 2.3) relies on species occurrence data, several ways to map the spatial distribution of ecosystem services have been developed (see Burkhard & Maes, 2017). The most simplistic approaches translate land cover data into ES maps using expert-based lookup tables (Burkhard et al., 2009; Jacobs et al., 2015). Other methods derive spatial explicit indicators from physical ES models. Participatory mapping approaches with a geographic information system (PGIS) ask individuals or groups of stakeholders to indicate areas on a map of particularly high ES supply or demand (Brown & Fagerholm, 2015; Palomo et al., 2012; Arslan & Örucü, 2020; Yoshimura & Hiura, 2017; Sherrouse et al., 2014). PGIS approaches are effective methods to capture the holistic and symbolic, non-monetary values that ES provide to individuals or the society. Recent methods derive the distribution of ES values for larger areas of interest based on crowd-sourced data (Seda Arslan et al., 2021; Yoshimura & Hiura, 2017; Sherrouse et al., 2014). These methods use spatial regression or classification techniques with a range of independent landscape variables. A widely used tool to map social values of ecosystem services (SolVES; Sherrouse et al., 2014), combines spatial and non-spatial user input data. The spatially explicit output of PGIS approaches provides an important input for land use planning and decision-making processes. Here, such ES maps will be used to calculate the spatially explicit LCA endpoint impacts of wind energy (section 3.3) and the maps will ultimately be integrated into a wind energy planning tool, developed in another part of the project.

³ Biodiversity will not be mapped with the participatory approach since it is assessed in more detail in chapter 6.

Typically, individual responses from a PGIS are overlaid and merged to create averaged ES maps. However, to delineate areas of high ES value, averaging individual opinions might not capture the wide range of perspectives that could lead to opposition against wind energy projects. Therefore, we combine a spatial Delphi approach (Di Zio et al., 2017) with two rounds of mapping ecosystem services. Whereas classical spatial Delphi approaches aim to narrow down specific geographical locations for determining the best spots for a specific project or land-use (i.e. same location), our approach aims to narrow the geographic characteristics that provides ES (i.e. same *type* of location). Consequently, we expect that during the two mapping rounds of the spatial Delphi, people achieve a more common understanding regarding the optimal landscape configuration for high ES value. The resulting maps provide consensus-based ES maps of the study areas indicating areas where people expect high ES value to be found.

3.2.1 PGIS combined with spatial Delphi

The spatial Delphi approach developed here includes two participatory rounds (Figure 3). A detailed diagram of the procedures to map each ES in round one is shown in Figure 4. We implemented the tool in the R programming language as a web application based on R-shiny. On the server side, the application uses GOOGLE EARTH ENGINE (Gorelick et al., 2017) to assure performant and interactive spatial extrapolating of user data input (section 3.2.2). All the data and answers of the questionnaire are stored on server-based relational databases. Besides the core part of participatory ES mapping, the web application includes a questionnaire and a pairwise comparison of ecosystem services. In the second round, participants are given the opportunity to adjust their maps based on other participants' inputs from the first round. The grey boxes in figures 3 and 4 indicate the data output to be used for the spatial extrapolation of ES, the second Delphi round or within the impact calculation (section 3.3).

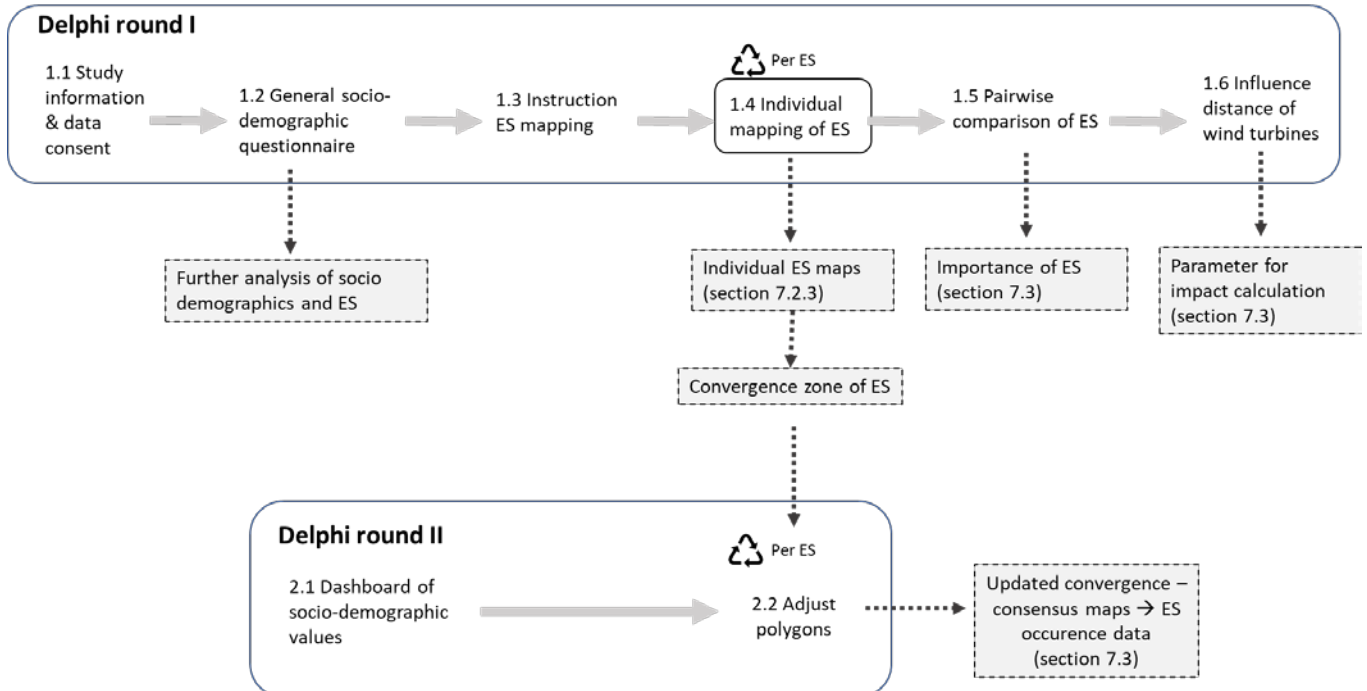


Figure 3: User interaction and data output (grey) of two spatial Delphi rounds.

In the first round, participants get information about the study content and information regarding the general data protection and regulation (GDPR) of personal data. To follow GDPR rules we generate a seven-digit random string as unique identifier (UID) for each participant to access the data in anonymized form. To be able to contact people for the second Delphi round, we ask for their e-mail address. However, this is completely on voluntary basis and if a participant does not provide the email, it is still possible to complete the first Delphi round. The data, containing the UID and email is stored outside the main database to ensure anonymity of the used data. The procedure starts with the presentation of the study area (Figure 5) and a subsequent questionnaire concerning peoples' socio-demographics (age, gender, education), statements to measure their environmental attitudes and questions regarding their familiarity with the study area. Before the mapping starts, the application provides a detailed instruction page containing a stepwise explanation of the mapping procedure. The system randomly selects four out of the ten ES to counterbalance and avoid fatigue effects in the mapping. Each selected ES is then mapped through the process outlined in Figure 4. We are aware, that it might be difficult or even impossible for people to indicate areas that provide a high value for some of the ecosystem services. Therefore, the mapping tool provides an opt-out and we can consider prepared expert-based ES mapping and modelling approaches for those specific ES (e.g. ARIES, Villa et al., 2014 or InVest, Sharp et al., 2020). The tool assures that participants draw their polygon training data inside the study area and that training polygons do not overlap.

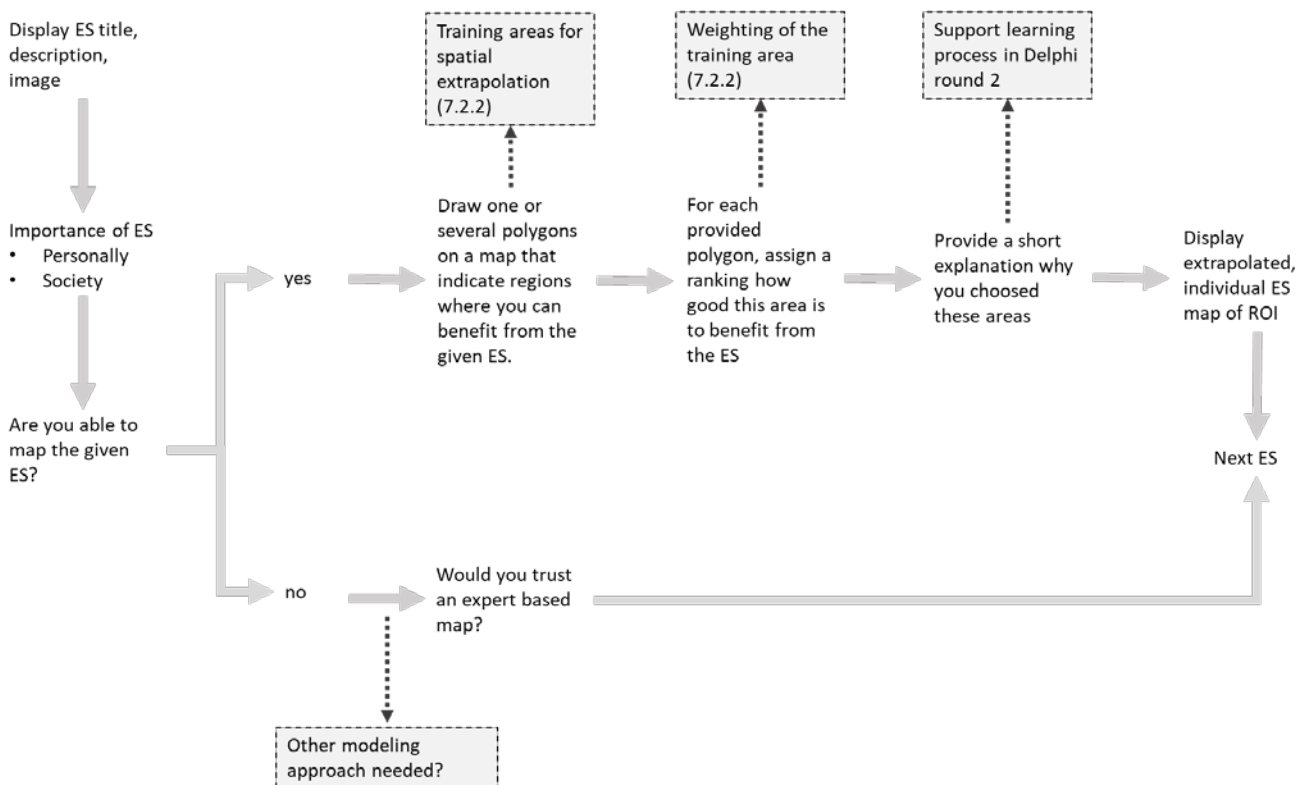


Figure 4: Detailed procedure and outputs (grey) of participatory mapping of each ES in round one of the spatial Delphi.

To immediately feedback the individual spatial distributions of the ES in the whole area, the polygons and ratings are used as training data for a maximum entropy (Maxent; Phillips et al., 2006) machine learning approach (section 3.2.2). The extrapolated ES maps are then used to calculate ES convergence zone maps (section 3.2.3).

After completing this mapping procedure for four ES, Delphi round one ends with a pairwise comparison of the importance of all ES within the study area. To reduce the total number of 45 pairs from ten ES, the application first asks for the pairwise comparison of the three CICES sections cultural, provisioning and regulating ES. Subsequently the comparison of the individual ES groups needs to be done only within each section. The pairwise comparison will be analysed with the analytic hierarchy process (AHP) and further used for the establishment of a net environmental performance indicator (see chapter 4). Finally, for the ES that are affected by visual and acoustic midpoint effects (Table 2), participants are asked to indicate how much their potential use of a good spot for a particular ES would be affected by visual impacts of wind turbines. For each of the ES this can be indicated with a slider that ranges from 0 (not affected at all) to 1 (complete useless to benefit from the ES in the area). Section 3.3 shows how these ratings will further be used in the calculation of the ES disturbance pathway in the LCA disturbance of wind energy.



WENDY POC mapping ecosystem services

About the study

Ecosystem services

Ecosystem services are services provided by nature. These services have a significant impact on the well-being and health of individuals. But the prosperity and welfare of entire societies also depend on well-functioning ecosystem services. Ecosystems and ecosystem services are affected by economic growth, population increase and changes in climatic conditions. Especially the development of settlements and infrastructures often negatively influences ecosystem services and thus has negative effects for all of us.

Why we need you

Not all ecosystem services occur in all areas equally. Their spatial distribution is a complex interaction of soil, air and water. However, to better protect important areas that provide ecosystem services from human interventions, we need to better understand where and which services humans benefit from nature. To find out where important areas for ecosystem services are, we need you. Because you know your homeland, its landscapes and the nature best. You can probably tell us something about many services of the landscape. The whole questionnaire will focus on the following study area:

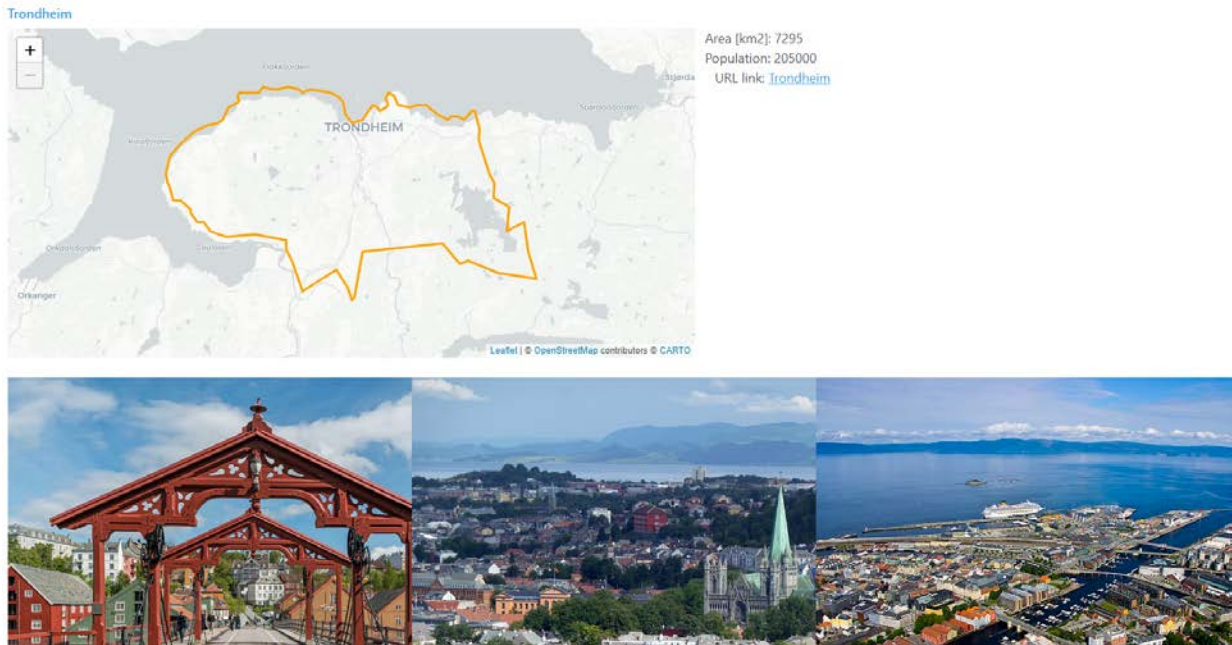


Figure 5: Screenshot of the introduction screen of the Spatial Delphi tool (9.8.23).

The second round of the spatial Delphi starts with a dashboard of general statistics about round one. Subsequently, participants can retrieve their individual ES maps, their polygons, and the convergence zone maps, for each of the four mapped ES in round one. In addition, participants see the anonymized explanation from other participants for their choice of specific ES areas. Based on this information, participants are asked to reconsider their polygons. Either participants decide not to change their selection of good areas for ES or they can adjust their polygons. In the same way as in round one, the system calculates the individual ES maps and the updated convergence zone maps for each ES. Thus, the spatial Delphi approach results in a more common understanding across participants which configuration of landscape variables (section 3.2.2) provides high levels of ES. In addition, the resulting consensus maps represent spatially explicit information of ES distribution in the study area. Similarly to the species distribution maps (section 2.3), the consensus based ES distribution maps serve as main input for the calculation of wind energy impacts on ecosystem services (section 3.3).

3.2.2 Spatial extrapolation of ecosystem services

Recent studies have applied maximum entropy distribution modelling (Maxent; Phillips et al., 2006) to predict ES probabilistic distribution in space (Seda Arslan et al., 2021; Yoshimura & Hiura, 2017; Sherrouse et al., 2014). Here we extrapolate the probability of ES occurrence in a study area, based on

user-defined polygons and methods which are related to species distribution modelling described in chapter 2. While species distribution models use species presence data, this approach uses the user polygons as the ES presence data and explanatory environmental variables (Table 3). For each participant, this leads to probability maps of valued ES areas covering the whole study area. Although extrapolation over large areas is technically possible, one should only extrapolate within areas of similar culture, since it has been shown that particularly valuations and perceptions of cultural ecosystem services are dependent on cultural backgrounds (Dou et al., 2020).

Study area

For this study we use the second level of the Global Administrative Unit Layers (GAUL; FAO UN) as target study area to map ecosystem service values. This globally available classification at level 2 represents district administrative boundaries and serves as the focal area for the subsequent impact assessment (3.3). For offshore wind energy sites, we define rectangles of 100x100 km to delineate the study boundaries.

Explanatory environmental variables

To apply the mapping tool within all WENDY European case study areas and to secure potential application in other areas, the minimal spatial extent of all explanatory variables is set to Europe.

Table 3: Independent, explanatory variables to predict distribution of ecosystem service benefits.

| Name | Description | Source | Values | Spatial resolution for MaxEnt | On-/offshore |
|------------------------------|---|---|--------------|-------------------------------|--------------|
| Ecosystem integrity (ON_INT) | Quantification of ecosystem integrity degradation. As a combined measure of human pressures on ecosystem structure, composition and function. | United Nations Environment Programme World Conservation Monitoring Centre (UNEP-WCMC) | 0 - 1 | 1000 m | Onshore |
| Topography (ON_DEM) | Copernicus DEM GLO-30: Global 30m Digital Elevation Model | Copernicus Digital Elevation Model - Copernicus Contributing Missions | 0 - 8900 [m] | 30 m | Onshore |



| | | | | | |
|---------------------------------|--|---|----------------|----------------------------|----------|
| Land use / Land cover (ON_LULC) | Copernicus CORINE Land Cover 2018 | Copernicus Land Monitoring Service | 1 - 45 | 100 m | Onshore |
| Accessibility (ON_ACC) | Cost surface of walking between street map layer. | Calculation of speeds according to open street layer. Burak et al., 2021. | 0 - 1 | 100 m | Onshore |
| Bathymetry (OFF_BAT) | ETOPO Global Relief Model 2022 | National Centers for Environmental Information | 0 – 12000 [m] | 1 arc minute ~810 – 1500 m | Offshore |
| Distance to coast (OFF_ACC) | Euclidean distance to coast line | | 0 – 500000 [m] | 1000 m | Offshore |
| Seabed substrate (OFF_LULC) | Classified seabed substrate types for European seas, representing seabed cover | ICES | 0 - 28 | 1000 m | Offshore |
| Inverse human impact (OFF_NAT) | Human pressures and impacts on marine ecosystem services | A Global Map of Human Impacts to Marine Ecosystems (ucsb.edu) | 0 - 1 | 935 m | Offshore |

The ecosystem integrity layer was provided by the World Conservation Monitoring Centre (UNEP-WCMC), based on Hill et al. (2022). Land- and seabed cover were retrieved from the international mapping authorities (Tab. 3). Topography and Bathymetry could be directly assessed via the data catalogue in GOOGLE EARTH ENGINE. Onshore accessibility has been calculated following the proposed method of Burak et al. (2021). Accessibility represents a cost surface of walking times between based on an open street map road network. Distance to coast has been calculated in R as a spatial raster layer.

Distribution of ecosystem service values

The Maxent algorithm has been implemented on GOOGLE EARTH ENGINE (Gorelick et al., 2017) and revealed comparable results compared to standalone MaxEnt software (Campos et al., 2023). As a widely applied representative of the *presence-background* model family, MaxEnt uses present points and samples of background points. The polygons provided by the study participants are treated as *ES presence data* while the rest of the study area is considered as background data, solely containing the



environmental variables. We sample the number of presence and background points relative to the polygon area (presence points) and the study area excluding the polygons (background points). In addition, we multiply the number of presence points with the corresponding ES value (1-5) the participants provided for each polygon. This emphasizes areas and thus landscape configurations that have been rated as of high value for a specific ES. Exemplary, Figure 6 shows two rectangles in a study area provided by the participant. The orange rectangle was valued as 5, the red as 2. Thus, the point density in red is double and in orange five times higher as in the surrounding area containing the background points.

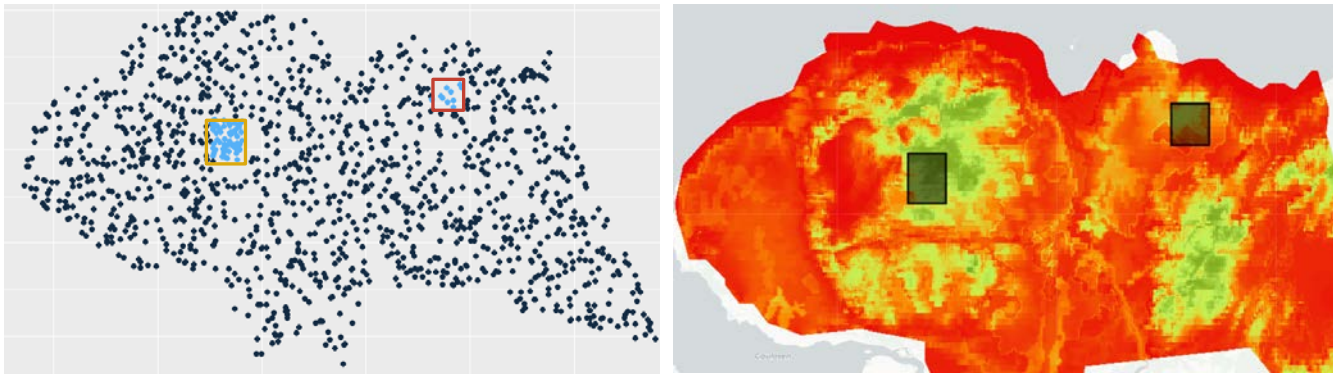


Figure 6: Point sampling strategy and corresponding Maxent extrapolation.

Figure 6 shows an example of the probability distribution to find areas of high ES quality for an individual participant based on Maxent. Green indicates areas with a high probability to find areas that provide the ecosystem service. Besides the individual distribution maps, we store the model performance AUC and variable importance for each participant. Within the mapping task, we ask people to draw polygons that delineates an area as precise as possible but are large enough to cover a certain amount of landscape variability to be able to extrapolate the probability to other areas. As soon as polygons remain smaller than the spatial resolution of the background data, the spatial variability of the background data in the polygons remains zero. Therefore, the mapping tool restricts the minimum and maximum zoom level to increase probability to draw large enough polygons. However, if the provided user polygon is still equal or even smaller than the spatial resolution of the explanatory data, the application only considers this polygon points as valuation data but not as training information.

3.2.3 Convergence zones of ecosystem services

After each spatial Delphi round, the convergence zones of a specific ES for all participants are calculated. These zones represent areas with lower level of dispersion around the mean ES values across individual participants. Dispersion is measured by the coefficient of variation (CV) from all participants within an ES. Hence after completing the Delphi rounds, the cellwise mean and standard deviation of each ES map based on all participants are calculated. The ratio of standard deviation to the mean finally results in the CV map. Areas of particularly low CV values (<1) are considered as convergence zones.

3.3 Integration of ESA into LCA

Accounting for the PDF of ecosystem services through wind energy infrastructure, we follow the same logic as the potential loss of species richness (PDF, section 2.5). In the ecosystem service context, the PDF represents a relative measure for the potential loss of ecosystem services through the loss of area induced by different impact pathways. Thus, at a given site represented by raster cell i , the area available to benefit from ES after the lost area follows $A_{new,i} = A_{org,i} - A_{lost,i}$. A_{lost} depends on the impact pathway (3.3.3 / 3.3.4) and $A_{org,i}$ represents the area of a single cell (and thereby the spatial resolution of the assessment). Compared to section 6.5 that uses the species-area relationship (SAR), this section applies the invariability-area relationship (IAR) as a measure of stability of an ecological variable over different scales (3.3.1; Wang et al., 2017). For each ecosystem service k , we account for two possible midpoint – endpoint impact pathways X ; disturbance and land occupation (Table 2). The potentially disappeared fraction (PDF) for an ecosystem service k and impact pathway X for wind farm f at cell i is given by

$$PDF(X)_{k,f,i} = \frac{IAR_{k,i} \left(1 - \left(\frac{A_{org,i} - A(X)_{lost,k,f,i}}{A_{org,i}} \right)^{z_k} \right)}{\sum_{i=1}^n IAR_{k,i}} \quad (4)$$

The estimation of the area lost for each cell in the raster, $A(X)_{lost,k,f,i}$, is given by the union of the impacted area for each wind turbine w (detailed expressions are given in section 6.5). The total PDF for ecosystem service k and impact pathway X at a wind farm f is the sum of all the cell-wise PDFs, $PDF(X)_{k,f} = \sum_i PDF(X)_{k,f,i}$. Most of the ecosystem services, in particular regulating and provisioning services, are affected through land occupation (Table 2). Area lost caused by land occupation (O) corresponds to the habitat loss in the biodiversity assessment (2.5.1). However, cultural ecosystem services are additionally affected within a wider area around wind turbines. Thus, for the midpoint *impact visual and acoustics*, we apply an area lost due to disturbance (D).

To ensure comparability of potential disappeared fraction (PDF) from the biodiversity and PDF from ecosystem services assessment, we harmonize the data as follows. Firstly, we ensure the use of the same spatial reference system ETRS89, LAEA (EPSG: 3035). Secondly, the spatial resolution (A_{orig}) of the ecosystem service assessment is resampled for onshore and offshore according to the spatial resolution of the biodiversity assessment (1 km² onshore and 10 km² offshore).

3.3.1 Invariability-area relationship (IAR)

Wang et al. (2017) proposed a relationship that measures stability or invariability of ecological variables in space over different spatial scales. Following the analogy of biodiversity with the species-area relationship, the stability of ecosystems services increases with larger areas. Consequently, ecosystem services in larger areas are more resilient to impacts, compared to small areas. The relationship between area and invariability (or stability) IAR has been shown as key to understand the scaling effects of ecological stability (Hodapp et al., 2023; Wang et al., 2017). The IAR represents the squared inverse of the coefficient of variation of an ecological variable and the spatial extent of the study area (Hodapp et al., 2023). We adapt this concept and use the IAR to account for ecosystem service values in the

considered area. IAR at a location i , for an ecosystem service k , is the reciprocal of the squared coefficient of variation CV (5).

$$IAR_{k,i} = \frac{1}{CV_{k,i}^2} \quad (5)$$

The coefficient of variation follows the standard formula $CV_{k,i}^2 = \frac{\sigma_{k,i}^2}{\mu_{k,i}^2}$. The squared variance (σ) and mean (μ) are calculated based on participants' individual ES probability maps from the second spatial Delphi round.

3.3.2 The z-value as the shape of IAR

The strength of spatial synchrony across different patches of an ecosystem service reflects the shape of IAR, i.e., the z value as the slope of the IAR vs. area on log-log scale (Wang et al., 2017; Hodapp et al., 2023). In the unrealistic case that all ES patches in the study area are spatially completely uncorrelated, z equals 1 on the $\log(IAR)$ - $\log(\text{area})$ scale. On the other hand, if all patches are perfectly correlated, IAR does not change with larger areas and $z = 0$ (Hodapp et al. 2023). Wang et al. (2017) showed two types of IAR-Area relationships. In our case we assume a power law decay of synchrony with increasing distances between sites. For a given site i and an ecosystem service k , we calculated $IAR_{k,i}$ and mean $IAR_{k,A}$ for increasing areas (A) surrounding i . We then derived $z_{k,i}$ as the slope of the linear \log_{10} - \log_{10} scaled invariability – area relationship (Figure 7). The average z_{k} over all $z_{k,i}$ is then used in equation 4 as case study specific z exponent.

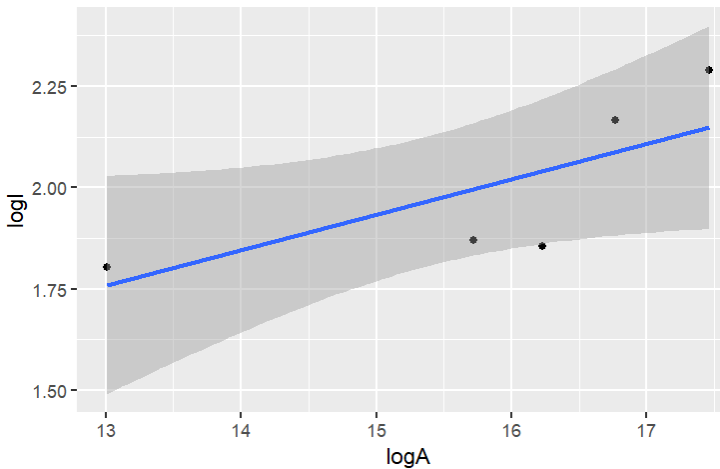


Figure 7: Example of log-log scaled invariability – area relationship.

3.3.3 Area lost for ecosystem services due to land occupation $A(O)$

Wind turbines need a certain area for the fundament construction, roads, transmission, substation, and permanent maintenance areas (Dehnholm et al., 2009). These constructions alter the land cover from natural areas to artificial surfaces. Consequently, the respective area is assumed as lost to gain ES values during the operational phase of a wind turbine. However, this does not directly imply an irreversible loss of the area for ES supply after the operational phase. As already shown in section 2.5.1 the area lost a_{EP} [km^2/MW] is a function of the wind turbine capacity (EP). For permanent constructions, we use $a_{EP} = 0.003 \text{ km}^2/\text{MW}$, for temporary occupation $a_{EP} = 0.007 \text{ km}^2/\text{MW}$ (NVE, 2022; Dehnholm et al.,

2009). Thus, the area lost for each ES for each wind turbine due to land occupation follows $A(O)_{lost,k,f,w} = a_{EP}EP_w$ (May et al., 2020).

3.3.4 Area lost for ecosystem services due to disturbance $A(D)$

Besides a smaller area which is completely occupied by the wind energy infrastructure, a wider area around the infrastructure is affected due to acoustic and visual effects. Like the disturbance in the biodiversity context (2.5.2), the area still provides ES but the beneficiaries might be disturbed since people avoid the area. In the area of visual or acoustic impact, we assume the disturbance as a function of distance to a wind turbine. We estimate the area lost due to disturbance for the respective ecosystem services k and for each wind turbine by $A(D)_{lost,k,f,w} = \pi(D_k d_{k,max})^2$ (May et al., 2020). The disturbance factor (D) follows

$D_k = \int_{d=0}^{d_{k,max}} \frac{1-1/1+e^{\beta(d-d_{k,max})}}{d_{k,max}} d\theta$ (May et al., 2020), where $\beta = \frac{\log((2-\alpha)/\alpha)}{d_{k,min}-\bar{d}_k}$ with $\alpha = 0.1$, $d_{k,min}$ as the minimum and \bar{d}_k the mean of disturbance distance d for ecosystem service k . $d_{k,min}$ and $d_{k,max}$ are derived from the distribution of ES(k) hotspots and thus specific for the study area. Firstly, for each ES hotspot areas where $CV_k < 1$ are identified. Secondly, for all the pixels (i) in the study area, the Euclidean distances to the hotspot pixels up to max 40km are calculated and transformed into a cumulative distribution function (CDF). From the first spatial Delphi round (section 3.2.1) all the user inputs regarding the probability that people will avoid an ES hotspot area is then used in the inverse CDF to obtain $d_{k,min}$ and $d_{k,max}$.

3.3.5 Weighted PDF for ecosystem services

In accordance with section 2.5 the total PDF for an ecosystem service k and wind farm f is given as the sum of all impact pathways X , $PDF_{k,f} = \sum_x PDF(X)_{k,f}$. The total PDF of a wind farm is then given by the weighted sum of the PDFs from the individual ecosystem services, $PDF_f = \sum_k w_k PDF_{k,f}$. The w_k 's are relative weights (summing to 1) of the different ecosystem services, which are assessed through the questionnaire of the first spatial Delphi round. Figure 3 shows that participants fulfil a pairwise comparison of the ecosystem services based on their individual perceived importance of a service within the study area. The pairwise comparison ranges from "A is much more important than B" to "both are equally important" and "B is much more important than A". To establish a hierarchy among importance of ecosystem services, we applied an analytic hierarchy process (AHP). Thus, we transformed the individual ratings into an individual, hierarchical importance matrix. After consistency checks, the individual importance weights are aggregated across all participants based on the eigenvalue method to get an overall importance weight for each ecosystem service, w_k .



4 Net environmental performance index

The obtained PDFs from both the biodiversity and ecosystem service assessment are finally integrated into a composite Key Performance Indicator (KPI). This KPI is a net environmental performance indicator (NEP) for a specific wind energy development site (wind farm). To calculate the NEP the total PDFs for biodiversity and ecosystem services will be normalized (0,1) to have measures which are comparable across regions and wind farms. This is done by subtracting the theoretical minimum PDFs and dividing by the theoretical maximum PDFs for the given wind farm (i.e. linear stretch). The maximum and minimum PDFs are calculated the same way as the actual PDFs (equations 1, 3 and 4), if the wind farm were to be positioned at the site with the maximum or minimum values of $S_k P_{k,i}$, $S_k C_{k,i}$ and $IAR_{k,i}$ that can be found in the focal region. Thus, we have $PDF_{B,f}^* = (PDF_{B,f} - PDF_{B,f,min}) / (PDF_{B,f,max} - PDF_{B,f,min})$ and $PDF_{ES,f}^* = (PDF_{ES,f} - PDF_{ES,f,min}) / (PDF_{ES,f,max} - PDF_{ES,f,min})$. Then the NEP is calculated as the mean of ecosystem service and biodiversity PDFs for the wind farm f .

$$NEP_f = 1 - (PDF_{ES,f}^* + PDF_{B,f}^*)0.5. \quad (5)$$

The NEP relies on both, the intrinsic (biodiversity) and the utilitarian (ecosystem services) value of nature, without emphasizing one or the other dimension. It gives an evaluation of the impact of a wind farm at a given site, relative to the range of possible impacts if the wind farm was sited elsewhere in the region of interest. Values close to 0 indicate a low environmental performance and that the wind farm is sited where there will be a strong combined impact on ecosystem services and biodiversity. As the distribution of PDFs may be skewed, knowledge of the central tendency will be important for the interpretation of the NEP. Thus, we also calculate the NEP for median PDFs, $NEP_{f,median} = 1 - (PDF_{ES,f,median}^* + PDF_{B,f,median}^*)0.5$. This allows the actual NEP to be evaluated relative to the NEP of a wind farm sited at a site with median impact on the environmental indicators. The NEP can also be scaled by the annual energy production to E_f [GW/yr] for the wind farm f , which is the (scaled) characterization factor for the LCA.

$$CF_f = NEP_f E_f^{-1} \quad (6)$$

Here E_f is a function of the wind turbine model (hub height, rotor diameter, capacity factor) and the spatially explicit wind conditions (wind speed distribution, loss factors, air density). The factor can also be estimated by multiplying the wind turbine or wind farm capacity (MW) with the expected full load hours per year, calculated as the total number of hours in a year (8760) times the capacity factor (e.g. 0.4). Thereafter this value can be divided by 1000 to obtain annual energy production in GWh/yr. The division by E_f makes the CF a relative measure, indicating the environmental performance per GWh produced. This LCA characterization factor enables offsetting impacts on biodiversity and ecosystem services against production. It allows the comparison of siting impacts across regions and/or wind farms.

5 Conclusion

Both intrinsic and utilitarian values of nature are sensitive to impacts caused by wind energy production. This report develops a conceptual framework for considering both aspects in spatial explicit manner for various impact pathways within an LCA. The intrinsic values of nature are represented with species occurrence maps accounting for all commonly found European species of birds, bats and marine mammals. Assessing the utilitarian values of nature is based on a novel approach, using a participatory mapping of ecosystem services. With an interactive spatial Delphi approach, stakeholders map areas of high ES benefits. Finally, both assessments calculate the impacts of wind energy infrastructure for different impact pathways as potential disappeared fraction (PDF) of species richness or ecosystem services. The rigorous use of the same impact calculation methods makes it possible to combine the impacts on biodiversity and ecosystem services into one single environmental performance indicator (NEP). The NEP gives a valuation of the site-specific impact of a wind farm, relative to other locations in a study area. Such an indicator is an easy-to-use KPI that supports planners and developers of wind farms as well as policy makers. Further the NEP can be combined with other KPI's. The tools, methods and calculation routines, developed in this conceptual stage will be further operationalized in other work packages and tasks in the WENDY project. For an exploitation outline including exploitation potential, intellectual property protection, potential exploitation pathways and partners' plans we refer to supplementary material Table S5.



6 References

- ABSG. (2021). Floating Offshore Wind Turbine Development Assessment: Final Report and Technical Summary. ABS Group.
- Anantharaman, R., Hall, K., Shah, V. B., & Edelman, A. (2020). Circuitscape in Julia: High Performance Connectivity Modelling to Support Conservation Decisions. *Proceedings of the JuliaCon Conferences*, 1(1), 58. <https://doi.org/10.21105/jcon.00058>
- Ancillotto, L., Bosso, L., Smeraldo, S., Mori, E., Mazza, G., Herkt, M., Galimberti, A., Ramazzotti, F., & Russo, D. (2020). An African bat in Europe, *Plecotus gaisleri*: Biogeographic and ecological insights from molecular taxonomy and Species Distribution Models. *Ecology and Evolution*, 10(12), 5785-5800. <https://doi.org/10.1002/ece3.6317>
- Assis, J., Tyberghein, L., Bosch, S., Verbruggen, H., Serrao, E. A., & De Clerck, O. (2018). Bio-ORACLE v2.0: Extending marine data layers for bioclimatic modelling. *Global Ecology and Biogeography*, 27(3), 277-284. <https://doi.org/10.1111/geb.12693>
- Barber, R. A., Ball, S. G., Morris, R. K. A., & Gilbert, F. (2022). Target-group backgrounds prove effective at correcting sampling bias in Maxent models. *Diversity and Distributions*, 28(1), 128-141. <https://doi.org/10.1111/ddi.13442>
- Bare, J. C., Hofstetter, P., Pennington, D. W., & de Haes, H. A. U. (2000). Life Cycle Impact Assessment Workshop Summary Midpoints versus Endpoints: The Sacrifices and Benefits. *International Journal of Life Cycle Assessment*, 5(6), 319-326. <https://doi.org/10.1007/Bf02978665>
- Barre, K., Le Viol, I., Bas, Y., Julliard, R., & Kerbiriou, C. (2018). Estimating habitat loss due to wind turbine avoidance by bats: Implications for European siting guidance. *Biological Conservation*, 226, 205-214. <https://doi.org/10.1016/j.biocon.2018.07.011>
- Bezanson, J., Edelman, A., Karpinski, S., & Shah, V. B. (2017). Julia: A Fresh Approach to Numerical Computing. *Siam Review*, 59(1), 65-98. <https://doi.org/10.1137/141000671>
- BirdLife International. (2021). European Red List of Birds. Publications Office of the European Union, Luxembourg
- Buchmayr, A., Verhofstadt, E., Van Ootegem, L., Thomassen, G., Taelman, S. E., & Dewulf, J. (2022). Exploring the global and local social sustainability of wind energy technologies: An application of a social impact assessment framework. *Applied Energy*, 312, 118808. <https://doi.org/10.1016/j.apenergy.2022.118808>
- Bjørge, A., Fagerheim, K.-A., Lydersen, C., Skern-Mauritzen, M., & Wiig, Ø. (2010). Marine mammals (Fisken og havet, special edition, Issue 2-2010).
- Brenda, P., Dietz, C., Andreas, M., Hotový, J., Lučan, R. K., Maltby, A., Meakin, K., Truscott, J., & Vallo, P. (2008). Bats (Mammalia: Chiroptera) of the Eastern Mediterranean and Middle East. Part 6. Bats of Sinai (Egypt) with some taxonomic, ecological and echolocation data on that fauna. *Acta Societas Zoologicae Bohemicae*, 72, 1-103.
- Brown, G., & Fagerholm, N. (2015). Empirical PPGIS/PGIS mapping of ecosystem services: A review and evaluation. *Ecosystem Services*, 13, 119–133. <https://doi.org/10.1016/J.ECOSER.2014.10.007>
- Burkhard, B., Kroll, F., Müller, F., & Windhorst, W. (2009). Landscapes' capacities to provide ecosystem



services - A concept for land-cover based assessments. *Landscape Online*, 15(1), 15–15. <https://doi.org/10.3097/LO.200915>

Burkhard, B., & Maes, J. (2017). Mapping Ecosystem Services. *Advanced Books*, 1, e12837-. <https://doi.org/10.3897/AB.E12837>

Callesen, I. (2016). Biodiversity and ecosystem services in life cycle impact assessment – Inventory objects or impact categories? *Ecosystem Services*, 22, 94–103. <https://doi.org/10.1016/J.ECOSER.2016.09.021>

Campos, J. C., Garcia, N., Alírio, J., Arenas-Castro, S., Teodoro, A. C., & Sillero, N. (2023). Ecological Niche Models using MaxEnt in Google Earth Engine: Evaluation, guidelines and recommendations. *Ecological Informatics*, 76, 102147. <https://doi.org/10.1016/J.ECOINF.2023.102147>

Collen, A. (2012). The evolution of echolocation in bats: a comparative approach [PhD Thesis, University College London]. London.

Correia, A. M., Sousa-Guedes, D., Gil, A., Valente, R., Rosso, M., Sousa-Pinto, I., Sillero, N., Pierce, G. J., Sillero, N., & Pierce, G. J. (2021). Predicting Cetacean Distributions in the Eastern North Atlantic to Support Marine Management. *Frontiers in Marine Science*, 8, 643569. <https://doi.org/10.3389/fmars.2021.643569>

Costanza, R. (2020). Valuing natural capital and ecosystem services toward the goals of efficiency, fairness, and sustainability. *Ecosystem Services*, 43, 101096. <https://doi.org/10.1016/J.ECOSER.2020.101096>

Dai, K. S., Bergot, A., Liang, C., Xiang, W. N., & Huang, Z. H. (2015). Environmental issues associated with wind energy - A review. *Renewable Energy*, 75, 911-921. <https://doi.org/10.1016/j.renene.2014.10.074>

de Boer, M. N., Clark, J., Leopold, M. F., Simmonds, M. P., & Reijnders, P. J. H. (2013). Photo-Identification Methods Reveal Seasonal and Long-Term Site-Fidelity of Risso's Dolphins (*Grampus griseus*) in Shallow Waters (Cardigan Bay, Wales). *Open Journal of Marine Science*, 3, 66-75. <https://doi.org/10.4236/ojms.2013.32A007>

De Luca Peña, L. V., Taelman, S. E., Prétat, N., Boone, L., Van der Biest, K., Custódio, M., Hernandez Lucas, S., Everaert, G., & Dewulf, J. (2022). Towards a comprehensive sustainability methodology to assess anthropogenic impacts on ecosystems: Review of the integration of Life Cycle Assessment, Environmental Risk Assessment and Ecosystem Services Assessment. *Science of The Total Environment*, 808, 152125. <https://doi.org/10.1016/J.SCITOTENV.2021.152125>

Denholm, P., Hand, M., Jackson, M., & Ong, S. (2009). Land-Use Requirements of modern wind power plants in the United States.

Dennis, R. L. H., & Thomas, C. D. (2000). Bias in butterfly distribution maps: the influence of hot spots and recorder's home range. *Journal of Insect Conservation*, 4(2), 73-77. <https://doi.org/10.1023/A:1009690919835>

Dierschke, V., Furness, R. W., & Garthe, S. (2016). Seabirds and offshore wind farms in European waters: Avoidance and attraction. *Biological Conservation*, 202, 59-68. <https://doi.org/10.1016/j.biocon.2016.08.016>



- Dietz, R., Teilmann, J., Andersen, S. M., Riget, F., & Olsen, M. T. (2013). Movements and site fidelity of harbour seals (*Phoca vitulina*) in Kattegat, Denmark, with implications for the epidemiology of the phocine distemper virus. *Ices Journal of Marine Science*, 70(1), 186-195. <https://doi.org/10.1093/icesjms/fss144>
- Di Zio, S., Castillo Rosas, J. D., & Lamelza, L. (2017). Real Time Spatial Delphi: Fast convergence of experts' opinions on the territory. *Technological Forecasting and Social Change*, 115, 143-154. <https://doi.org/10.1016/J.TECHFORE.2016.09.029>
- Dou, Y., Yu, X., Bakker, M., De Groot, R., Carsjens, G. J., Duan, H., & Huang, C. (2020). Analysis of the relationship between cross-cultural perceptions of landscapes and cultural ecosystem services in Genheyuan region, Northeast China. *Ecosystem Services*, 43, 101112. <https://doi.org/10.1016/J.ECOSER.2020.101112>
- Ellerbrok, J. S., Delius, A., Peter, F., Farwig, N., & Voigt, C. C. (2022). Activity of forest specialist bats decreases towards wind turbines at forest sites. *Journal of Applied Ecology*, 59(10), 2497-2506. <https://doi.org/10.1111/1365-2664.14249>
- Engler, J. O., Stiels, D., Schidelko, K., Strubbe, D., Quillfeldt, P., & Brambilla, M. (2017). Avian SDMs: current state, challenges, and opportunities. *Journal of Avian Biology*, 48(12), 1483-1504. <https://doi.org/10.1111/jav.01248>
- Fick, S. E., & Hijmans, R. J. (2017). WorldClim 2: new 1-km spatial resolution climate surfaces for global land areas. *International Journal of Climatology*, 37(12), 4302-4315. <https://doi.org/10.1002/joc.5086>
- Foley, H. J., Pacifici, K., Baird, R. W., Webster, D. L., Swaim, Z. T., & Read, A. J. (2021). Residency and movement patterns of Curviers beaked whales. *Marine Ecology Progress Series*, 660, 203-216. <https://doi.org/10.3354/meps13593>
- Fourcade, Y., Engler, J. O., Rodder, D., & Secondi, J. (2014). Mapping Species Distributions with MAXENT Using a Geographically Biased Sample of Presence Data: A Performance Assessment of Methods for Correcting Sampling Bias. *Plos One*, 9(5), e97122. <https://doi.org/10.1371/journal.pone.0097122>
- Frey-Ehrenbold, A., Bontadina, F., Arlettaz, R., & Obrist, M. K. (2013). Landscape connectivity, habitat structure and activity of bat guilds in farmland-dominated matrices. *Journal of Applied Ecology*, 50(1), 252-261. <https://doi.org/10.1111/1365-2664.12034>
- Froidevaux, J. S. P., Toshkova, N., Barbaro, L., Benitez-Lopez, A., Kerbiriou, C., Le Viol, I., Pacifici, M., Santini, L., Stawski, C., Russo, D., Dekker, J., Alberdi, A., Amorim, F., Ancillotto, L., Barre, K., Bas, Y., Cantu-Salazar, L., Dechmann, D. K. N., Devaux, T., . . . Razgour, O. (2023). A species-level trait dataset of bats in Europe and beyond. *Scientific Data*, 10, 253. <https://doi.org/10.1038/s41597-023-02157-4>
- Furness, R. W., Wade, H. M., & Masden, E. A. (2013). Assessing vulnerability of marine bird populations to offshore wind farms. *Journal of Environmental Management*, 119, 56-66. <https://doi.org/10.1016/j.jenvman.2013.01.025>
- Gaultier, S. P., Lilley, T. M., Vesterinen, E. J., & Brommer, J. E. (2023). The presence of wind turbines repels bats in boreal forests. *Landscape and Urban Planning*, 231, 104636. <https://doi.org/10.1016/j.landurbplan.2022.104636>



- Genov, T., Bearzi, G., Bonizzoni, S., & Tempesta, M. (2012). Long-distance movement of a lone short-beaked common dolphin *Delphinus delphis* in the central Mediterranean Sea. *Marine Biodiversity Records*, 5, e9. <https://doi.org/10.1017/S1755267211001163>
- Gomez, C., Lawson, J. W., Wright, A. J., Buren, A. D., Tollit, D., & Lesage, V. (2016). A systematic review on the behavioural responses of wild marine mammals to noise: the disparity between science and policy. *Canadian Journal of Zoology*, 94(12), 801-819. <https://doi.org/10.1139/cjz-2016-0098>
- Gorelick, N., Hancher, M., Dixon, M., Ilyushchenko, S., Thau, D., & Moore, R. (2017). *Google Earth Engine: Planetary-scale geospatial analysis for everyone*. <https://doi.org/10.1016/j.rse.2017.06.031>
- Grenie, M., Violle, C., & Munoz, F. (2020). Is prediction of species richness from stacked species distribution models biased by habitat saturation? *Ecological Indicators*, 111, 105970. <https://doi.org/10.1016/j.ecolind.2019.105970>
- Haines-Young, R., Potschin, M., & others. (2010). The links between biodiversity, ecosystem services and human well-being. *Ecosystem Ecology: A New Synthesis*, 1, 110–139.
- Haines-Young, R., Potschin, M. (2018). Common International Classification of Ecosystem Services (CICES) V5.1 and Guidance on the Application of the Revised Structure? Available from www.cices.eu. Fabis Consulting Ltd, The Paddocks, Chestnut Lane, Barton in Fabis, Nottingham, NG11 0AE, UK.
- Hardaker, A., Styles, D., Williams, P., Chadwick, D., & Dandy, N. (2022). A framework for integrating ecosystem services as endpoint impacts in life cycle assessment. *Journal of Cleaner Production*, 370, 133450. <https://doi.org/10.1016/J.JCLEPRO.2022.133450>
- Hedenstöm, A., Johansson, L. C., & Spedding, G. R. (2009). Bird or bat: comparing airframe design and flight performance. *Bioinspiration & Biomimetics*, 4, 015001. <https://doi.org/10.1088/1748-3182/4/1/015001>
- Hodapp, D., Armonies, W., Dannheim, J., Downing, J. A., Filstrup, C. T., & Hillebrand, H. (2023). Individual species and site dynamics are the main drivers of spatial scaling of stability in aquatic communities. *Frontiers in Ecology and Evolution*, 11, 864534. <https://doi.org/10.3389/FEVO.2023.864534>
- Holderied, M. W., Korine, C., Fenton, M. B., Parsons, S., Robson, S., & Jones, G. (2005). Echolocation call intensity in the aerial hawking bat *Eptesicus bottae* (Vespertilionidae) studied using stereo videogrammetry. *Journal of Experimental Biology*, 208(7), 1321-1327. <https://doi.org/10.1242/jeb.01528>
- Holland, R. A., Waters, D. A., & Rayner, J. M. V. (2004). Echolocation signal structure in the Megachiropteran bat *Rousettus aegyptiacus* Geoffroy 1810. *Journal of Experimental Biology*, 207(25), 4361-4369. <https://doi.org/10.1242/jeb.01288>
- Hutterer, R., Ivanova, T., Meyer-Cords, C., & Rodrigues, L. (2005). Bat migration in Europe: A review of banding data and literature. Federal Agency for Nature Conservation, Germany.
- IEA, Renewables (2022). IEA, Paris <https://www.iea.org/reports/renewables-2022>, License: CC BY 4.0
- Jaberg, C., & Guisan, A. (2001). Modelling the distribution of bats in relation to landscape structure in a temperate mountain environment. *Journal of Applied Ecology*, 38(6), 1169-1181. <https://doi.org/10.1046/j.0021-8901.2001.00668.x>



- Jacobs, S., Burkhard, B., Van Daele, T., Staes, J., & Schneiders, A. (2015). 'The Matrix Reloaded': A review of expert knowledge use for mapping ecosystem services. *Ecological Modelling*, 295, 21–30. <https://doi.org/10.1016/j.ecolmodel.2014.08.024>
- Jones, K. E., Bielby, J., Cardillo, M., Fritz, S. A., O'Dell, J., Orme, D. L., Safi, K., Sechrest, W., Boakes, E. H., Carbone, C., Connolly, C., Cutts, M. J., Foster, J. K., Grenyer, R., Habib, M., Plaster, C. A., Price, S. A., Rigby, E. A., Rist, J., . . . Purvis, A. (2009). PanTHERIA: a species-level database of life history, ecology, and geography of extant and recently extinct mammals. *Ecology*, 90(9), 2648. <https://doi.org/10.1890/08-1494.1>
- Kadmon, R., Farber, O., & Danin, A. (2004). Effect of roadside bias on the accuracy of predictive maps produced by bioclimatic models. *Ecological Applications*, 14(2), 401-413. <https://doi.org/10.1890/02-5364>
- Kettemer, L. E., Rikardsen, A. H., Biuw, M., Broms, F., Mul, E., & Blanchet, M.-A. (2022). Round-trip migration and energy budget of a breeding female humpback whale in the Northeast Atlantic. *Plos One*, 17(5), e0268355. <https://doi.org/10.1371/journal.pone.0268355>
- Landau, V. A., Shah, V. B., Anantharaman, R., & Hall, K. R. (2021). Omniscape.jl: Software to compute omnidirectional landscape connectivity. *Journal of Open Source Software*, 6(57), 2829. <https://doi.org/10.21105/joss.02829>
- Leroux, C., Kerbirou, C., Le Viol, I., Valet, N., & Barre, K. (2022). Distance to hedgerows drives local repulsion and attraction of wind turbines on bats: Implications for spatial siting. *Journal of Applied Ecology*, 59(8), 2142-2153. <https://doi.org/10.1111/1365-2664.14227>
- Lunde, T. H., Roksvaag, T. B., & Solheim, S. (2021). Mooring of Floating Offshore Wind Turbines: A review of the mooring designs and the installation vessels for floating offshore wind turbines [Bachelor thesis, Norwegian University of Science and Technology]. Trondheim.
- Lydersen, C., Vacquie-Garcia, J., Heide-Jorgensen, M. P., Oien, N., Guinet, C., & Kovacs, K. M. (2020). Autumn movements of fin whales (*Balaenoptera physalus*) from Svalbard, Norway, revealed by satellite tracking. *Scientific Reports*, 10(1), 16966. <https://doi.org/10.1038/s41598-020-73996-z>
- Ma, K.-T., Luo, Y., Kwan, T., & Wu, Y. (2019). Mooring System Engineering for Offshore Structures. Elsevier. <https://doi.org/10.1016/C2018-0-02217-3>
- Matthews, C. J. D., Luque, S. P., Petersen, S. D., Andrews, R. D., & Ferguson, S. H. (2011). Satellite tracking of a killer whale (*Orcinus orca*) in the eastern Canadian Arctic documents ice avoidance and rapid, long-distance movement into the North Atlantic. *Polar Biology*, 34(7), 1091-1096. <https://doi.org/10.1007/s00300-010-0958-x>
- Maxwell, S. M., Kershaw, F., Locke, C. C., Conners, M. G., Dawson, C., Aylesworth, S., Loomis, R., & Johnson, A. F. (2022). Potential impacts of floating wind turbine technology for marine species and habitats. *Journal of Environmental Management*, 307, 114577. <https://doi.org/10.1016/j.jenvman.2022.114577>
- May, R., Jackson, C. R., Middel, H., Stokke, B. G., & Verones, F. (2021). Life-cycle impacts of wind energy development on bird diversity in Norway. *Environmental Impact Assessment Review*, 90, 106635. <https://doi.org/10.1016/j.eiar.2021.106635>



- May, R., Middel, H., Stokke, B. G., Jackson, C., & Verones, F. (2020). Global life-cycle impacts of onshore wind-power plants on bird richness. *Environmental and Sustainability Indicators*, 8, 100080. <https://doi.org/10.1016/j.indic.2020.100080>
- McConnell, B. J., Fedak, M. A., Lovell, P., & Hammond, P. S. (1999). Movements and foraging areas of grey seals in the North Sea. *Journal of Applied Ecology*, 36(4), 573-590. <https://doi.org/10.1046/j.1365-2664.1999.00429.x>
- McNab, B. K. (2008). An analysis of the factors that influence the level and scaling of mammalian BMR. *Comparative Biochemistry and Physiology, Part A*, 151(1), 5-28. <https://doi.org/10.1016/j.cbpa.2008.05.008>
- McRae, B. H., Dickson, B. G., Keitt, T. H., & Shah, V. B. (2008). Using Circuit Theory to Model Connectivity in Ecology, Evolution, and Conservation. *Ecology*, 89(10), 2712-2724. <https://doi.org/10.1890/07-1861.1>
- McRae, B. H., Popper, K., Jones, A., Schindel, M., Buttrick, S., Hall, K. R., Unnasch, R. S., & Platt, J. (2016). Conserving nature's stage: Mapping omnidirectional connectivity for resilient terrestrial landscapes in the pacific northwest. T. N. Conservancy. nature.org/resilienceNW
- Michaelsen, T. C. (2016). Summer temperature and precipitation govern bat diversity at northern latitudes in Norway. *Mammalia*, 80(1), 1-9. <https://doi.org/10.1515/mammalia-2014-0077>
- Miller, P. J. O., Kvadsheim, P. H., Lam, F. P. A., Tyack, P. L., Cure, C., DeRuiter, S. L., Kleivane, L., Sivle, L. D., van IJsselmuide, S. P., Visser, F., Wensveen, P. J., von Benda-Beckmann, A. M., Lopez, L. M. M., Narazaki, T., & Hooker, S. K. (2015). First indications that northern bottlenose whales are sensitive to behavioural disturbance from anthropogenic noise. *Royal Society Open Science*, 2(6), 140484. <https://doi.org/10.1098/rsos.140484>
- Minderman, J., Gillis, M. H., Daly, H. F., & Park, K. J. (2017). Landscape-scale effects of single- and multiple small wind turbines on bat activity. *Animal Conservation*, 20(5), 455-462. <https://doi.org/10.1111/acv.12331>
- Nawojchik, R., St Aubin, D. J., & Johnson, A. (2003). Movements and dive behavior of two stranded, rehabilitated long-finned pilot whales (*Globicephala melas*) in the Northwest Atlantic. *Marine Mammal Science*, 19(1), 232-239. <https://doi.org/10.1111/j.1748-7692.2003.tb01105.x>
- Obrist, M. K., Boesch, R., & Fluckiger, P. F. (2004). Variability in echolocation call design of 26 Swiss bat species: consequences, limits and options for automated field identification with a synergetic pattern recognition approach. *Mammalia*, 68(4), 307-322. <https://doi.org/10.1515/mamm.2004.030>
- Olsen, E., Budgell, P., Head, E., Kleivane, L., Nøttestad, L., Prieto, R., Silva, M. A., Skov, H., Vikingsson, G. A., Waring, G., & Øien, N. (2009). First Satellite-Tracked Long-Distance Movement of a Sei Whale (*Balaenoptera borealis*) in the North Atlantic. *Aquatic Mammals*, 35(3), 313-318. <https://doi.org/10.1578/AM.35.3.2009.313>
- Palomo, I., Martín-Ló Pez, B., Potschin, M., Haines-Young, R., & Montes, C. (2012). *National Parks, buffer zones and surrounding lands: Mapping ecosystem service flows*. <https://doi.org/10.1016/j.ecoser.2012.09.001>
- Phillips, S. B., Aneja, V. P., Kang, D., & Arya, S. P. (2006). Maximum entropy modeling of species geographic distributions. *Ecological Modelling*, 190(3-4), 231-259.



<https://doi.org/10.1016/J.ECOLMODEL.2005.03.026>

- Phillips, S. J., Anderson, R. P., Dudik, M., Schapire, R. E., & Blair, M. E. (2017). Opening the black box: an open-source release of Maxent. *Ecography*, 40(7), 887-893. <https://doi.org/10.1111/ecog.03049>
- Phillips, S. J., Dudik, M., Elith, J., Graham, C. H., Lehmann, A., Leathwick, J., & Ferrier, S. (2009). Sample selection bias and presence-only distribution models: implications for background and pseudo-absence data. *Ecological Applications*, 19(1), 181-197. <https://doi.org/10.1890/07-2153.1>
- Picchi, P., van Lierop, M., Geneletti, D., & Stremke, S. (2019). Advancing the relationship between renewable energy and ecosystem services for landscape planning and design: A literature review. *Ecosystem Services*, 35, 241–259. <https://doi.org/10.1016/J.ECOSER.2018.12.010>
- Rasmussen, M. H., Akamatsu, T., Teilmann, J., Vikiugsson, G., & Miller, L. A. (2013). Biosonar, diving and movements of two tagged white-beaked dolphin in Icelandic waters. *Deep-Sea Research II*, 88-89, 97-105. <https://doi.org/10.1016/j.dsr2.2012.07.011>
- Read, A. J., & Westgate, A. J. (1997). Monitoring the movements of harbour porpoises (*Phocoena phocoena*) with satellite telemetry. *Marine Biology*, 130(2), 315-322. <https://doi.org/10.1007/s002270050251>
- Reid, J. B., Evans, P. G. H., & Northridge, S. P. (2003). Atlas of Cetacean distribution in north-west European waters. Joint Nature Conservation Committee.
- Robinson, K. P., O'Brien, J. M., Berrow, S. D., Cheney, B., Costa, M., Eisfeld, S. M., Haberlin, D., Mandleberg, L., O'Donovan, M., Oudejans, M. G., Ryan, C., Stevick, P. T., Thompson, P. M., & Whooley, P. (2012). Discrete or not so discrete: Long distance movements by coastal bottlenose dolphins in UK and Irish waters. *Journal of Cetacean Research and Management*, 12, 365-371. <https://doi.org/10.47536/jcrm.v12i3.569>
- Rugani, B., Maia de Souza, D., Weidema, B. P., Bare, J., Bakshi, B., Grann, B., Johnston, J. M., Pavan, A. L. R., Liu, X., Laurent, A., & Verones, F. (2019). Towards integrating the ecosystem services cascade framework within the Life Cycle Assessment (LCA) cause-effect methodology. *Science of the Total Environment*, 690, 1284–1298. <https://doi.org/10.1016/J.SCITOTENV.2019.07.023>
- Sampson, K., Merigo, C., Lagueux, K., Rice, J., Cooper, R., Weber, E. S., Kass, P., Mandelman, J., & Innis, C. (2012). Clinical assessment and postrelease monitoring of 11 mass stranded dolphins on Cape Cod, Massachusetts. *Marine Mammal Science*, 28(4), E404-E425. <https://doi.org/10.1111/j.1748-7692.2011.00547.x>
- Scherrer, D., Christe, P., & Guisan, A. (2019). Modelling bat distributions and diversity in a mountain landscape using focal predictors in ensemble of small models. *Diversity and Distributions*, 25(5), 770-782. <https://doi.org/10.1111/ddi.12893>
- Seda Arslan, E., Ömer, ., & Örüçü, K. (2021). *MaxEnt modelling of the potential distribution areas of cultural ecosystem services using social media data and GIS*. 23, 2655–2667. <https://doi.org/10.1007/s10668-020-00692-3>
- Sharp, R., Douglass, J., Wolny, S., Arkema, K., Bernhardt, J., Bierbower, W., Chaumont, N., Denu, D., Fisher, D., Glowinski, K., & others. (2020). InVEST 3.8. 7. User's Guide. *The Natural Capital Project, Stanford University, University of Minnesota, The Nature Conservancy, and World Wildlife Fund:*



Stanford, CA, USA.

- Sherrouse, B. C., Semmens, D. J., & Clement, J. M. (2014). An application of Social Values for Ecosystem Services (SolVES) to three national forests in Colorado and Wyoming. *Ecological Indicators*, 36, 68–79. <https://doi.org/10.1016/J.ECOLIND.2013.07.008>
- Smol, M. (2022). Is the green deal a global strategy? Revision of the green deal definitions, strategies and importance in post-COVID recovery plans in various regions of the world. *Energy Policy*, 169, 113152. <https://doi.org/10.1016/J.ENPOL.2022.113152>
- Somveille, M., Rodrigues, A. S. L., & Manica, A. (2018). Energy efficiency drives the global seasonal distribution of birds. *Nature Ecology & Evolution*, 2(6), 962-969. <https://doi.org/10.1038/s41559-018-0556-9>
- Southall, B. L., Bowles, A. E., Ellison, W. T., Finneran, J. J., Gentry, R. L., Greene, C. R., Jr., Kastak, D., Ketten, D. R., Miller, J. H., Nachtigall, P. E., Richardson, W. J., Thomas, J. A., & Tyack, P. L. (2007). Marine mammal noise exposure criteria: initial scientific recommendations. *Aquatic Mammals*, 33(4), 407-521. <https://doi.org/10.1578/AM.33.4.2007.411>
- Southall, B. L., Finneran, J. J., Riechmuth, C., Nachtigall, P. E., Ketten, D. R., Bowles, A. E., Ellison, W. T., Nowacek, D. P., & Tyack, P. L. (2019). Marine Mammal Noise Exposure Criteria: Updated Scientific Recommendations for Residual Hearing Effects. *Aquatic Mammals*, 45(2), 125-232. <https://doi.org/10.1578/Am.45.2.2019.125>
- Stahl Olafsson, A., Purves, R. S., Wartmann, F. M., Garcia-Martin, M., Fagerholm, N., Torralba, M., Albert, C., Verbrugge, L. N. H., Heikinheimo, V., Plieninger, T., Bieling, C., Kaaronen, R., Hartmann, M., & Raymond, C. M. (2022). Comparing landscape value patterns between participatory mapping and geolocated social media content across Europe. *Landscape and Urban Planning*, 226, 104511. <https://doi.org/10.1016/J.LANDURBPLAN.2022.104511>
- Stavenow, J., Roos, A. M., Ågren, E. O., Kinze, C., Englund, W. F., & Neimanis, A. (2022). Sowerby's Beaked Whales (*Mesoplodon bidens*) in the Skagerrak and Adjacent Waters: Historical Records and Recent Post-Mortem Findings. *Oceans*, 3, 250-267. <https://doi.org/10.3390/oceans3030018>
- Steiner, L., Lamoni, L., Plata, M. A., Jensen, S. K., Lettevall, E., & Gordon, J. (2012). A link between male sperm whales, *Physeter macrocephalus*, of the Azores and Norway. *Journal of the Marine Biological Association of the United Kingdom*, 92(8), 1751-1756. <https://doi.org/10.1017/S0025315412000793>
- Storch, D., Keil, P., & Jetz, W. (2012). Universal species-area and endemics-area relationships at continental scales. *Nature*, 488(7409), 78-81. <https://doi.org/10.1038/nature11226>
- Stöber, U., & Thomsen, F. (2021). How could operational underwater sound from future offshore wind turbines impact marine life? *Journal of the Acoustical Society of America*, 149(3), 1791-1795. <https://doi.org/10.1121/10.0003760>
- Thaxter, C. B., Buchanan, G. M., Carr, J., Butchart, S. H. M., Newbold, T., Green, R. E., Tobias, J. A., Foden, W. B., O'Brien, S., & Pearce-Higgins, J. W. (2017). Bird and bat species' global vulnerability to collision mortality at wind farms revealed through a trait-based assessment. *Proceedings of the Royal Society B*, 284(1862), 20170829. <https://doi.org/10.1098/rspb.2017.0829>



- Tjørve, E., Matthews, T. J., & Whittaker, R. J. (2021). The History of the Species–Area Relationship. In T. J. Matthews, K. A. Triantis, & R. J. Whittaker (Eds.), *The Species–Area Relationship: Theory and Application*. Cambridge University Press. <https://doi.org/10.1017/9781108569422.005>
- Tobias, J. A., Sheard, C., Pigot, A. L., Devenish, A. J. M., Yang, J. Y., Sayol, F., Neate-Clegg, M. H. C., Alioravainen, N., Weeks, T. L., Barber, R. A., Walkden, P. A., MacGregor, H. E. A., Jones, S. E. I., Vincent, C., Phillips, A. G., Marples, N. M., Montano-Centellas, F. A., Leandro-Silva, V., Claramunt, S., . . . Schleuning, M. (2022). AVONET: morphological, ecological and geographical data for all birds. *Ecology Letters*, 25(3), 581-597. <https://doi.org/10.1111/ele.13898>
- Torres-Florez, J. P., Olson, P. A., Bedrinana-Romano, L., Rosenbaum, H. C., Ruiz, J., LeDuc, R., & Hucke-Gaete, R. (2015). First documented migratory destination for eastern South Pacific bluewhales. *Marine Mammal Science*, 31(4), 1580-1586. <https://doi.org/10.1111/mms.12239>
- Tougaard, J., Hermanssen, L., & Madsen, P. T. (2020). How loud is the underwater noise from operating offshore wind turbines? *Journal of the Acoustical Society of America*, 148(5), 2885-2893. <https://doi.org/10.1121/10.0002453>
- Tyberghein, L., Verbruggen, H., Pauly, K., Troupin, C., Mineur, F., & De Clerck, O. (2012). Bio-ORACLE: a global environmental dataset for marine species distribution modelling. *Global Ecology and Biogeography*, 21(2), 272-281. <https://doi.org/10.1111/j.1466-8238.2011.00656.x>
- Verones, F., Bare, J., Bulle, C., Frischknecht, R., Hauschild, M., Hellweg, S., Henderson, A., Jolliet, O., Laurent, A., Liao, X., Lindner, J. P., de Souza, D. M., Michelsen, O., Patouillard, L., Pfister, S., Posthuma, L., Prado, V., Ridoutt, B., Rosenbaum, R. K., . . . Fantke, P. (2017). LCIA framework and cross-cutting issues guidance within the UNEP-SETAC Life Cycle Initiative. *Journal of Cleaner Production*, 161, 957-967. <https://doi.org/10.1016/j.jclepro.2017.05.206>
- Vikingsson, G. A., & Heide-Jørgensen, M. P. (2015). First indications of autumn migration routes and destination of common minke whales tracked by satellite in the North Atlantic during 2001-2011. *Marine Mammal Science*, 31(1), 376-385. <https://doi.org/10.1111/mms.12144>
- Villa, F., Bagstad, K. J., Voigt, B., Johnson, G. W., Portela, R., Honzák, M., & Batker, D. (2014). A Methodology for Adaptable and Robust Ecosystem Services Assessment. *PLOS ONE*, 9(3), e91001. <https://doi.org/10.1371/JOURNAL.PONE.0091001>
- Vincze, O., Vagasi, C. I., Pap, P. L., Palmer, C., & Moller, A. P. (2019). Wing morphology, flight type and migration distance predict accumulated fuel load in birds. *Journal of Experimental Biology*, 222(1), jeb183517. <https://doi.org/10.1242/jeb.183517>
- Wade, H. M., Masden, E. A., Jackson, A. C., & Furness, R. W. (2016). Incorporating data uncertainty when estimating potential vulnerability of Scottish seabirds to marine renewable energy developments. *Marine Policy*, 70, 108-113. <https://doi.org/10.1016/j.marpol.2016.04.045>
- Wang, S., Loreau, M., Arnoldi, J. F., Fang, J., Rahman, K. A., Tao, S., & De Mazancourt, C. (2017). An invariability-area relationship sheds new light on the spatial scaling of ecological stability. *Nature Communications*, 8(May), 1–8. <https://doi.org/10.1038/ncomms15211>
- Wiatros-Motyka, M., Jones, D., Broadbent, H., Fulghum, N., Bruce-Lockhart, C., Dizon, R., MacDonald, P., Moore, C., Candlin, A., Lee, U., Copsey, L., Hawkins, S., Ewen, M., Worthington, B., Benham, H.,



- Trueman, M., Yang, M., Lolla, A., Edianto, A. S., . . . Black, R. (2023). Global Electricity Review 2023. Ember. <https://ember-climate.org/insights/research/global-electricity-review-2023/>
- Williams, T. M. (1999). The evolution of cost efficient swimming in marine mammals: limits to energetic optimization. *Philosophical Transactions of the Royal Society B*, 354(1380), 193-201. <https://doi.org/10.1098/rstb.1999.0371>
- Yoshimura, N., & Hiura, T. (2017). Demand and supply of cultural ecosystem services: Use of geotagged photos to map the aesthetic value of landscapes in Hokkaido. *Ecosystem Services*, 24, 68–78. <https://doi.org/10.1016/J.ECOSER.2017.02.009>



7 Supplementary material

Table S1: Functional groups for all 545 species of birds which regularly occur in Europe. Groups are formed on the basis of functional similarity of the species and their taxonomic relationship. Some families of songbirds are represented in two groups and the non-passerines group are a miscellaneous group with families having only a few species each.

| Functional group | Number of species | Families represented |
|-------------------------|-------------------|--|
| Corvids | 17 | Corvidae, Laniidae |
| Gallinaceous birds | 25 | Turnicidae, Phasianidae, Otidae, Pteroclididae |
| Gulls | 30 | Laridae |
| Herbivorous songbirds | 57 | Calcariidae, Emberizidae, Fringillidae, Passeridae, Prunellidae |
| Insectivorous songbirds | 89 | Acrocephalidae, Aegithalidae, Alaudidae, Cisticolidae, Hirundinidae, Leiotrichidae, Locustellidae, Motacillidae, Muscicapidae, Panuridae, Paridae, Phylloscopidae, Regulidae, Remizidae, Scotocercidae, Sittidae |
| Non-passerines | 38 | Upupidae, Apodidae, Caprimulgidae, Columbidae, Alcedinidae, Coraciidae, Meropidae, Cuculidae, Picidae |
| Owls | 16 | Strigidae, Tytonidae |
| Polyphagous songbirds | 72 | Bombycillidae, Certhiidae, Cinclidae, Muscicapidae, Oriolidae, Prunellidae, Pycnonotidae, Sittidae, Sturnidae, Sylviidae, Troglodytidae, Turdidae |
| Raptors | 40 | Accipitridae, Elanidae, Pandionidae, Falconidae |
| Seabirds | 30 | Alcidae, Stercorariidae, Hydrobatidae, Oceanitidae, Procellariidae, Phalacrocoracidae, Sulidae |
| Waders | 52 | Burhinidae, Charadriidae, Glareolidae, Haematopodidae, Recurvirostridae, Scolopacidae |
| Waterbirds | 38 | Ciconiidae, Gaviidae, Gruidae, Rallidae, Ardeidae, Pelecanidae, Threskiornithidae, Phoenicopteridae, Podicipedidae, Anhingidae |
| Waterfowl | 41 | Anatidae |



Table S2: Species of bats which are found in Europe according to EUROBATS. Bats are classified based on the duration and bandwidth of echolocation calls into short-range echolocators (SRE), mid-range echolocators (MRE) and long-range echolocators (LRE). * = When no data for a species was found available echolocation call structure was assumed based on the calls of species in its genus. **The species is diurnal and frugivorous; thus, it also depends on vision for navigation.

| Scientific name | Echolocation call structure | Scientific name | Echolocation call structure |
|----------------------------------|-----------------------------|----------------------------------|-----------------------------|
| <i>Rousettus aegyptiacus</i> | SRE** | <i>Myotis mystacinus</i> | SRE |
| <i>Taphozous nudiventris</i> | LRE | <i>Myotis nattereri</i> | SRE |
| <i>Rhinolophus blasii</i> | SRE | <i>Myotis punicus</i> | SRE |
| <i>Rhinolophus euryale</i> | SRE | <i>Myotis schaubi</i> | SRE |
| <i>Rhinolophus ferrumequinum</i> | SRE | <i>Myotis tschuliensis</i> | SRE* |
| <i>Rhinolophus hipposideros</i> | SRE | <i>Nyctalus azoreum</i> | LRE |
| <i>Rhinolophus mehelyi</i> | SRE | <i>Nyctalus lasiopterus</i> | LRE |
| <i>Barbastella barbastellus</i> | SRE | <i>Nyctalus leisleri</i> | LRE |
| <i>Barbastella caspica</i> | SRE* | <i>Nyctalus noctula</i> | LRE |
| <i>Eptesicus anatolicus</i> | LRE* | <i>Otonycteris hemprichii</i> | MRE |
| <i>Eptesicus isabellinus</i> | LRE | <i>Pipistrellus hanaki</i> | MRE* |
| <i>Eptesicus nilssonii</i> | LRE | <i>Pipistrellus kuhlii</i> | MRE |
| <i>Eptesicus ognevi</i> | LRE | <i>Pipistrellus maderensis</i> | MRE |
| <i>Eptesicus serotinus</i> | LRE | <i>Pipistrellus nathusii</i> | MRE |
| <i>Hypsugo savii</i> | MRE | <i>Pipistrellus pipistrellus</i> | MRE |
| <i>Myotis alcathoe</i> | SRE | <i>Pipistrellus pygmaeus</i> | MRE |
| <i>Myotis bechsteinii</i> | SRE | <i>Plecotus auritus</i> | SRE |
| <i>Myotis blythii</i> | SRE | <i>Plecotus austriacus</i> | SRE |
| <i>Myotis brandtii</i> | SRE | <i>Plecotus gaisleri</i> | SRE* |
| <i>Myotis capaccinii</i> | SRE | <i>Plecotus kolombatovici</i> | SRE |
| <i>Myotis crypticus</i> | SRE* | <i>Plecotus macrobullaris</i> | SRE |
| <i>Myotis dasycneme</i> | SRE | <i>Plecotus sardus</i> | SRE |
| <i>Myotis daubentonii</i> | SRE | <i>Plecotus teneriffae</i> | SRE |
| <i>Myotis davidii</i> | SRE* | <i>Vespertilio murinus</i> | LRE |
| <i>Myotis emarginatus</i> | SRE | <i>Miniopterus pallidus</i> | MRE* |
| <i>Myotis escaleraei</i> | SRE | <i>Miniopterus schreibersii</i> | MRE |
| <i>Myotis hovei</i> | SRE* | <i>Tadarida teniotis</i> | LRE |
| <i>Myotis myotis</i> | SRE | | |

Table S3: Species of marine mammals (orders Cetacea and Carnivora) which are found the North Sea and along Norway in the Norwegian economic zone (Bjørge 2010, Reid 2013). Each species is assigned to a hearing group according to the current knowledge of their audiograms (Southall et al. 2019) and a group based on the taxonomy and functional similarity of species.

| Scientific name | Hearing group | Group |
|-----------------------------------|---------------|----------------|
| <i>Balaenoptera acutorostrata</i> | LF | Baleen whales |
| <i>Balaenoptera borealis</i> | LF | Baleen whales |
| <i>Balaenoptera musculus</i> | LF | Baleen whales |
| <i>Balaenoptera physalus</i> | LF | Baleen whales |
| <i>Megaptera novaeangliae</i> | LF | Baleen whales |
| <i>Physeter macrocephalus</i> | HF | Toothed whales |
| <i>Mesoplodon bidens</i> | HF | Toothed whales |
| <i>Ziphius cavirostris</i> | HF | Toothed whales |
| <i>Hyperoodon ampullatus</i> | HF | Toothed whales |
| <i>Lagenorhynchus albirostris</i> | HF | Toothed whales |
| <i>Lagenorhynchus acutus</i> | HF | Toothed whales |
| <i>Grampus griseus</i> | HF | Toothed whales |
| <i>Tursiops truncatus</i> | HF | Toothed whales |
| <i>Delphinus delphis</i> | HF | Toothed whales |
| <i>Orcinus orca</i> | HF | Toothed whales |
| <i>Globicephala melas</i> | HF | Toothed whales |
| <i>Phocoena phocoena</i> | VHF | Toothed whales |
| <i>Phoca vitulina</i> | PCW | Seals |
| <i>Halichoerus grypus</i> | PCW | Seals |

Table S4: Parameters for the marine mammal auditory weighting function for each of found hearing groups. LF = low-frequency cetaceans, HF = high-frequency cetaceans, VHF = very high-frequency cetaceans and PCW = phocid carnivores in water. Parameter estimates are from Southall et al. (2019).

| Marine mammal hearing group | f_1 (kHz) | f_2 (kHz) | a | b | C (dB) |
|-----------------------------|-------------|-------------|-----|-----|----------|
| LF | 0.20 | 19 | 1.0 | 2.0 | 0.13 |
| HF | 8.80 | 110 | 1.6 | 2.0 | 1.20 |
| VHF | 12.00 | 140 | 1.8 | 2.0 | 1.36 |
| PCW | 1.90 | 30 | 1.0 | 2.0 | 0.75 |

Table S5: Exploitation outline for the use of the results provided on the integrated life-cycle assessment of ecosystem services and biodiversity.

| | Dimensions | Analysis |
|---|-------------------------------|--|
| 1 | Exploitation potential | The main users of the tool are: - Wind energy developers |

| | Dimensions | Analysis |
|---|---|--|
| | | <p>With a given policy framework, the developer can use the spatially explicit information about biodiversity and ecosystem services in the scoping process to delineate sites with low environmental conflicts. The inclusion of ecosystem service values can additionally augment local acceptance of the project.</p> <ul style="list-style-type: none"> - National, regional, and local planning authorities and decision makers <p>The planning policies and guidelines can promote holistic siting approaches and spatially assess expected environmental impact of wind energy infrastructure for licensing. The approach can also contribute to Strategic Environmental Assessment for the identification of potentially suitable sites for wind energy development.</p> <p>The deliverable helps to understand and incorporate the social-ecological dimension into wind energy planning to foster sustainable energy development.</p> <p>Attractive, unique features described in the report are:</p> <ul style="list-style-type: none"> - Spatially explicit information regarding biodiversity and ecosystem services. - Combination of biodiversity and ecosystem service assessment within a Life Cycle Impact Assessment framework. - A comparable net environmental performance (NEP) index incorporating both ecosystem service and biodiversity impacts. - A novel approach to engage general public or other stakeholder groups into the mapping of ecosystem service benefits. |
| 2 | Intellectual property protection | <ul style="list-style-type: none"> - The (use of the) tool will need adhere to General Data Protection Regulations (GDPR). - The methodology operationalized in the tool will be used for further development internally, as well as used for providing a service to potential clients. - In principle, the methodology, tool and associated codes and routines will be published Open Source following EU regulations. |
| 3 | Potential exploitation pathways | <p>Exploitation actions could include, among others, the following:</p> <ul style="list-style-type: none"> • Incorporate the biodiversity and ecosystem service mapping into a framing application (web app or similar). • Process and code review of the application. • Define infrastructure to run the application and store the data. • Develop a rigorous user guide (handbook). • Promote the tool in scientific and professional communities. • Further development of research through other funding opportunities. |
| 4 | Partners' plans | <p>The proof of concept, as an outcome of this deliverable, forms the basis for further development of the tool to support holistic planning of wind energy</p> |

| | Dimensions | Analysis |
|--|------------|--|
| | | <p>infrastructure. The tool can be combined or incorporated into already developed decision support systems at NINA.</p> <p>In addition, the streamlined routines to map biodiversity and the participatory mapping of ecosystem services can support other research projects.</p> |

